Bridge between QCD and LFQM

Chueng-Ryong Ji
North Carolina State University

The 2nd CENuM Workshop for Hadron Physics

CENuM

Inha Hadron Theory Group

December 18, 2023

Outline

- **Motivation with 50-years QCD**
- **Global QCD Analysis of Hadron Structure**
- **Hadron Tomography in JLab and EIC**
- **Interpolation between IFD and LFD**
- **‘tHooft model as a toy QCD-LFQM bridge**
- **Hadron spectroscopy and wavefunctions**
- **Application to hadron physics**

How do we understand the Quark Model in Quantum Chromodynamics?

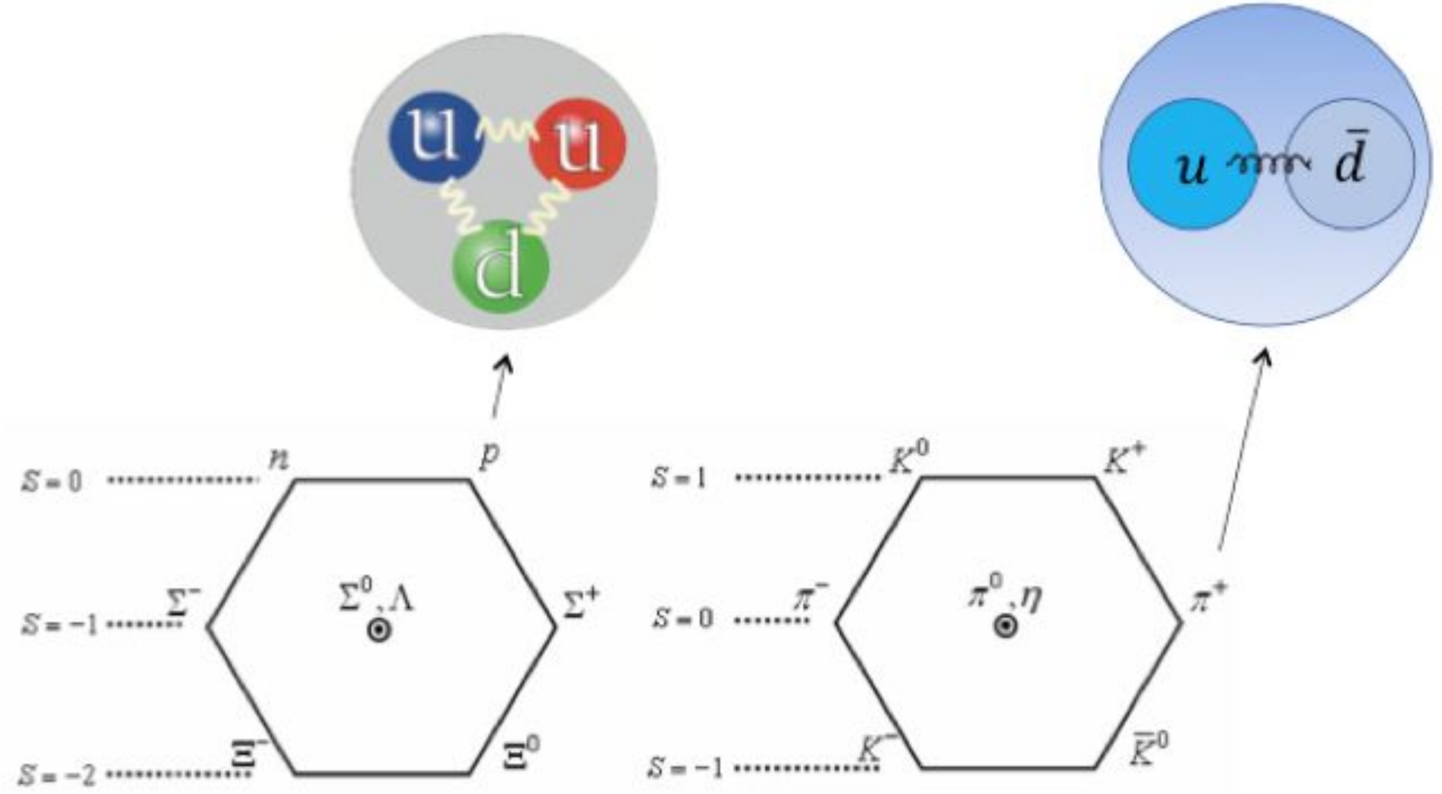

$$M_p = 938.272046 \pm 0.000021\, MeV$$

$$M_n = 939.565379 \pm 0.000021\, MeV$$

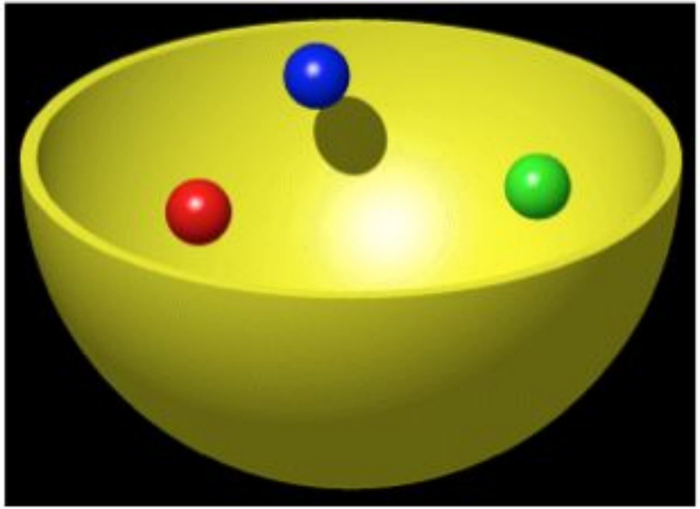

$\Longrightarrow$

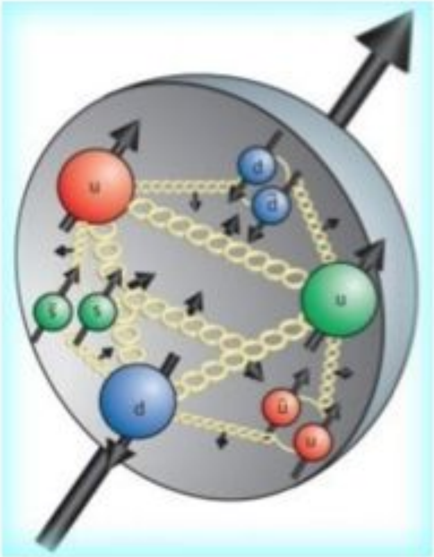

$$m_u = 2.3^{+0.7}_{-0.5}\ MeV \quad ; \quad m_d = 4.8^{+0.7}_{-0.3}\ MeV$$

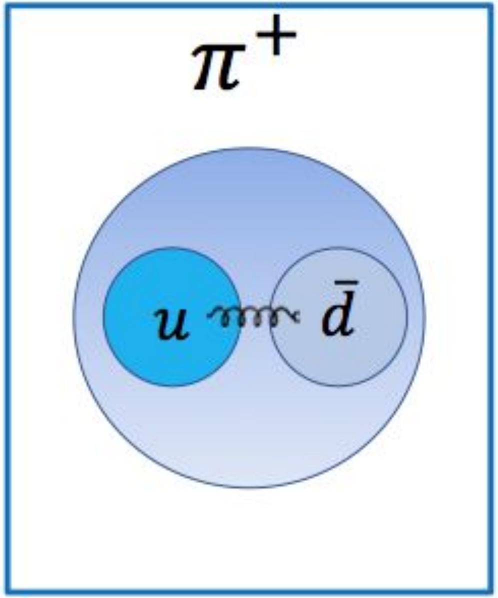

vs.

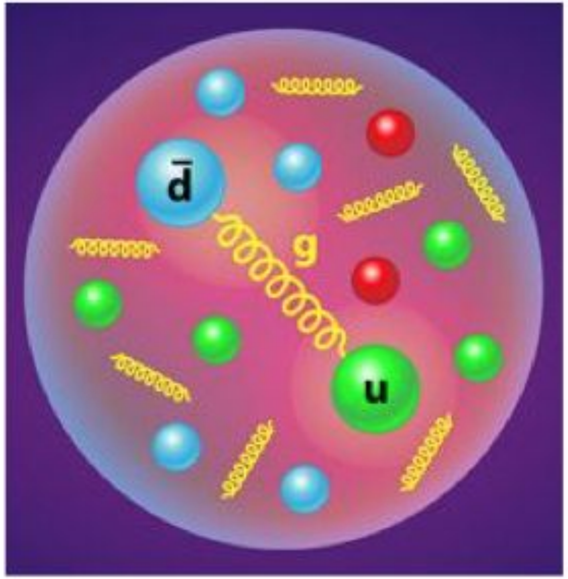

Constituent Quark Model

$$M = m_1 + m_2 + A\frac{\vec{s}_1 \cdot \vec{s}_2}{m_1 m_2}$$

$$m_u = m_d = 310 MeV/c^2$$

$$A = \left(\frac{2m_u}{\hbar}\right)^2 160 MeV/c^2$$

Quantum Chromodynamics

Isospin symmetry

Chiral symmetry

$\mathrm{SU}(2)_\mathrm{R} \times \mathrm{SU}(2)_\mathrm{L}$

Spontaneous symmetry breakdown

Goldstone Bosons

$F_\pi^2 M_\pi^2 = -(m_u + m_d)\langle 0|\bar{u}u|0\rangle$

Effective field theory

Goldstone-theorem

If the Lagrangian is invariant under a **continuous global** symmetry operation $g \in G$ and the vacuum is invariant under a subgroup $H \subset G$, then there exist $n(G/H) = n(G) - n(H)$ **massless spinless particles**.

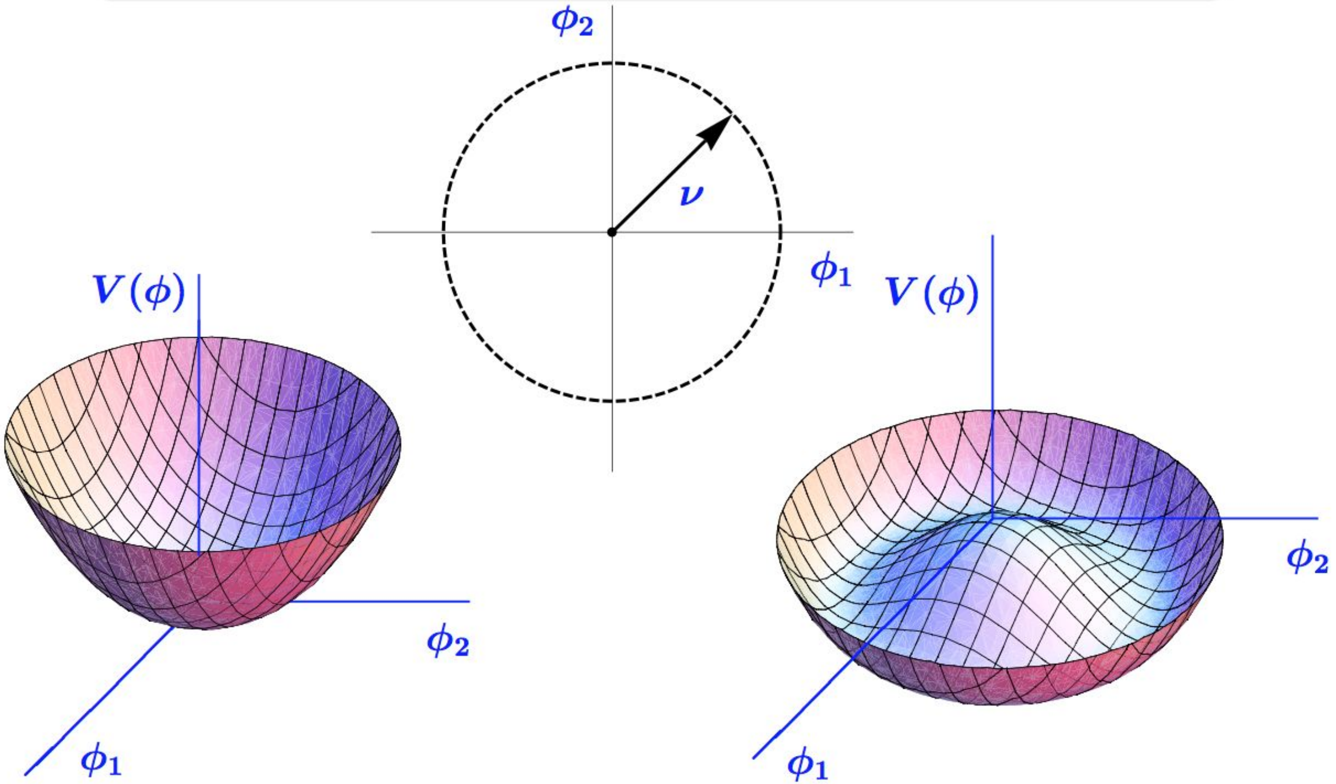

https://journals.aps.org/collections/50-years-QCD

50 Years of QCD

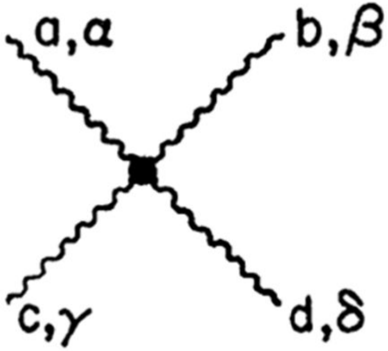

By 1973, there was growing interest in explaining the nature of the strong force via the gauge theory Quantum Chromodynamics (QCD). Three papers published that year—two in a June 1973 issue of *Physical Review Letters*, and one in the November 1973 issue of *Physical Review D*—demonstrated that such non-Abelian (*i.e.*, noncommutative) gauge theories are "asymptotically free," meaning that the coupling constant becomes smaller at high-energy scales. This key result implies that high-energy QCD processes are perturbatively calculable, and that at low energy the coupling becomes large, in agreement with the observed confinement of quarks.

To mark the 50th anniversary of this significant development in particle and nuclear physics, the editors of the *Physical Review* journals have curated a collection of landmark papers appearing in our journals. The papers trace key developments in QCD leading up to 1973, and some of the many discoveries since.

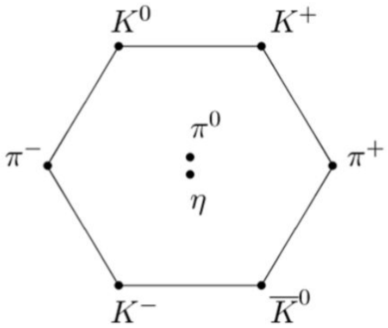

The pions, kaons and eta meson are organized in an octet arrangement according to the eightfold-way. I, Laurascudder, CC BY-SA 3.0

Towards QCD

The discovery of new hadrons, beyond the usual protons and neutrons that make up atomic nuclei, led to an ever increasing number of particles that were all thought to be elementary. An arrangement of hadrons according to the representations of the SU(3) group—the eightfold-way—provided a successful organizational principle for this intractable particle zoo, and predicted the existence of the omega baryon (discovered in 1964). This mathematical construct precipitated the hypothesis that three types of elementary particles called quarks (up, down, and strange) are the main constituents of these hadrons. An ensuing problem in satisfying the spin-statistics theorem while constructing certain hadrons called for a new quantum number, called "color", to be carried by the hypothetical quarks.

https://journals.aps.org/collections/50-years-QCD

Precision determination of parton distribution functions:

New parton distributions for collider physics

Hung-Liang Lai, Marco Guzzi, Joey Huston, Zhao Li, Pavel M. Nadolsky, Jon Pumplin, and C.-P. Yuan

Phys. Rev. D **82**, 074024 (2010)

Determination of the Strange-Quark Density of the Proton from ATLAS Measurements of the $W \to \ell\nu$ and $Z \to \ell\ell$ Cross Sections

G. Aad *et al*. (ATLAS Collaboration)

Phys. Rev. Lett. **109**, 012001 (2012)

First Monte Carlo Global QCD Analysis of Pion Parton Distributions

P.C. Barry, N. Sato, W. Melnitchouk, and Chueng-Ryong Ji (Jefferson Lab Angular Momentum (JAM) Collaboration)

Phys. Rev. Lett. **121**, 152001 (2018)

PHYSICAL REVIEW LETTERS **121,** 152001 (2018)

Featured in Physics

First Monte Carlo Global QCD Analysis of Pion Parton Distributions

P. C. Barry,[1] N. Sato,[2] W. Melnitchouk,[3] and Chueng-Ryong Ji[1]

(Jefferson Lab Angular Momentum (JAM) Collaboration)

[1]*North Carolina State University, Raleigh, North Carolina 27607, USA*
[2]*University of Connecticut, Storrs, Connecticut 06269, USA*
[3]*Jefferson Lab, Newport News, Virginia 23606, USA*

PHYSICAL REVIEW LETTERS **127,** 232001 (2021)

Global QCD Analysis of Pion Parton Distributions with Threshold Resummation

P. C. Barry,[1] Chueng-Ryong Ji,[2] N. Sato,[1] and W. Melnitchouk[1]

(JAM Collaboration)

[1]*Jefferson Lab, Newport News, Virginia 23606, USA*
[2]*Department of Physics, North Carolina State University, Raleigh, North Carolina 27695, USA*

Pion Properties

- Lightest bound state composed of quarks, antiquarks, and gluons
- Masses: $m_{\pi^\pm} = 139.57 \text{ MeV}, m_{\pi^0} = 134.977 \text{ MeV}$
- Lifetimes: $\tau_{\pi^\pm} = 2.603\times10^{-8} \text{ s}, \tau_{\pi^0} = 8.52\times10^{-17} \text{ s}$

Charged pions decay via weak interaction

Neutral pions decay via electromagnetic interaction, *i.e.* $\pi^0 \rightarrow \gamma\gamma$

Drell-Yan (DY)

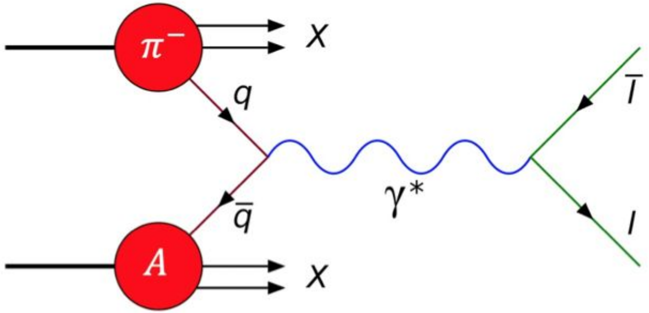

Leading Neutron (LN)

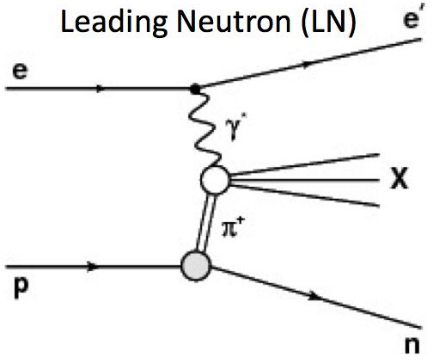

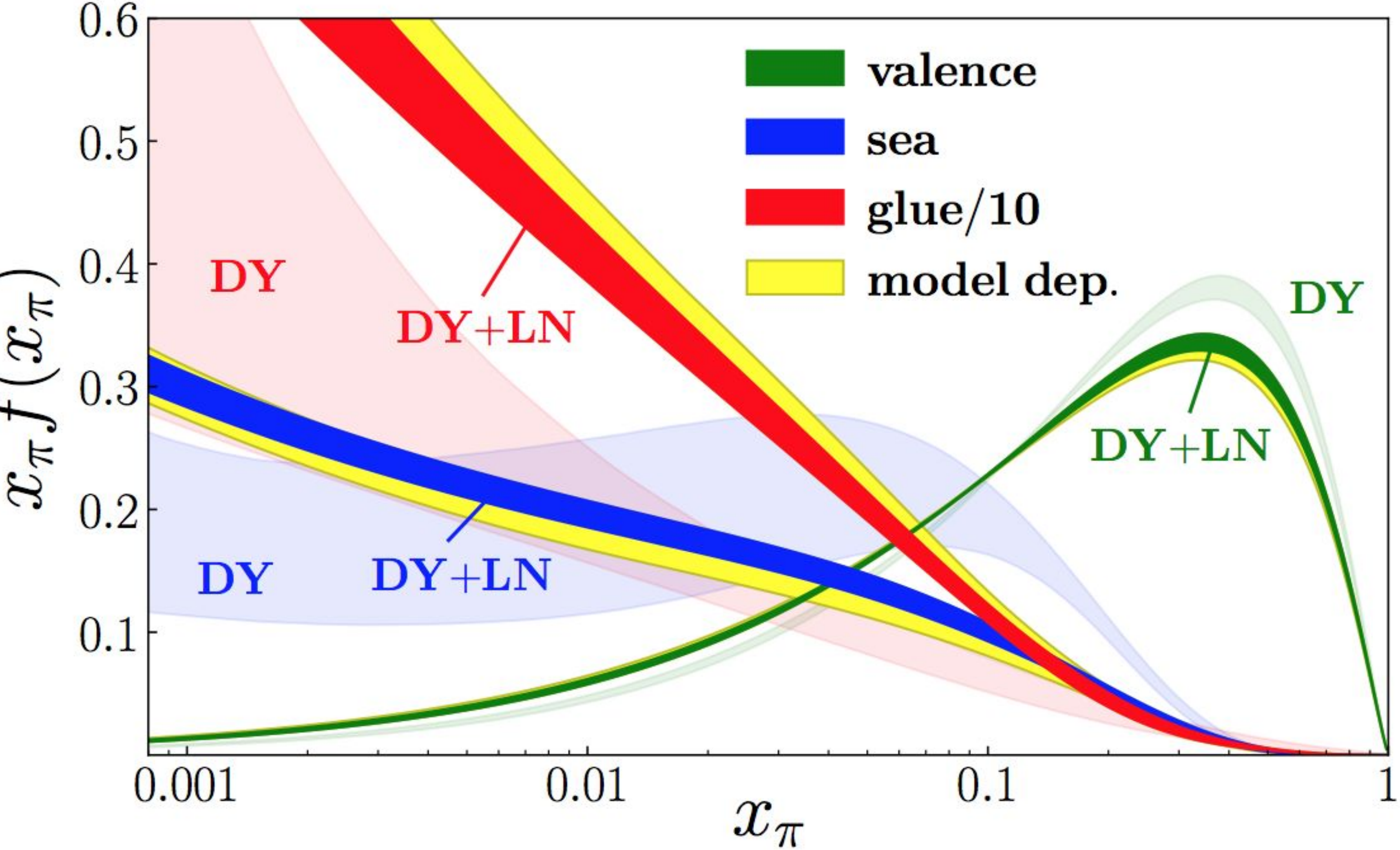
valence
sea
glue/10
model dep.
DY
DY+LN
DY
DY+LN
DY
DY+LN
0.6
0.5
0.4
0.3
0.2
0.1
0.001
0.01
0.1
1
$x_\pi f(x_\pi)$
x_π

Sea of the proton

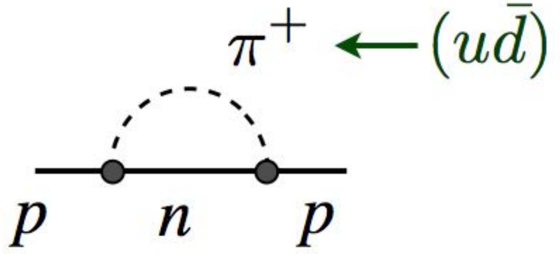

$\rightarrow \quad \bar{d} > \bar{u}$

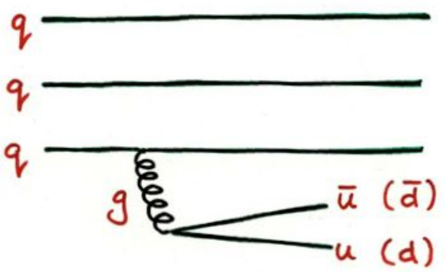

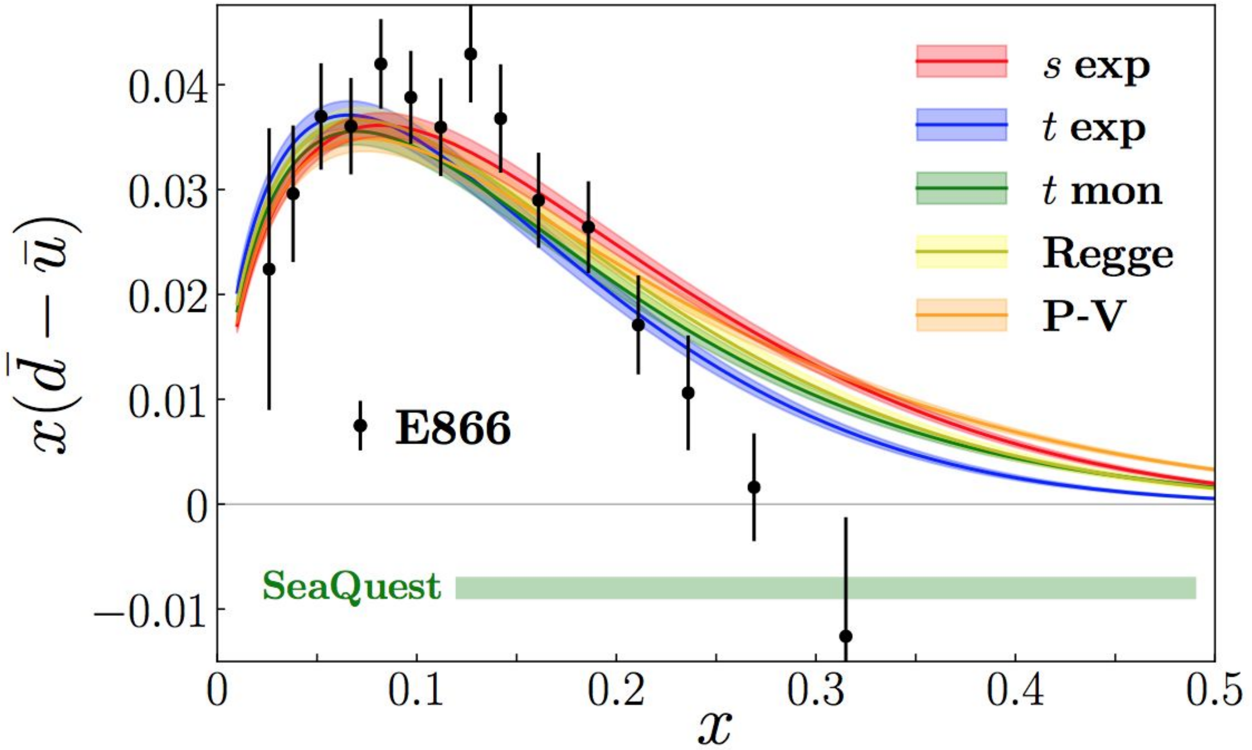

$$f_i(x, \mu_0; \boldsymbol{a}_i) = N_i x^{\alpha_i} (1-x)^{\beta_i} (1 + \gamma_i x^2)$$

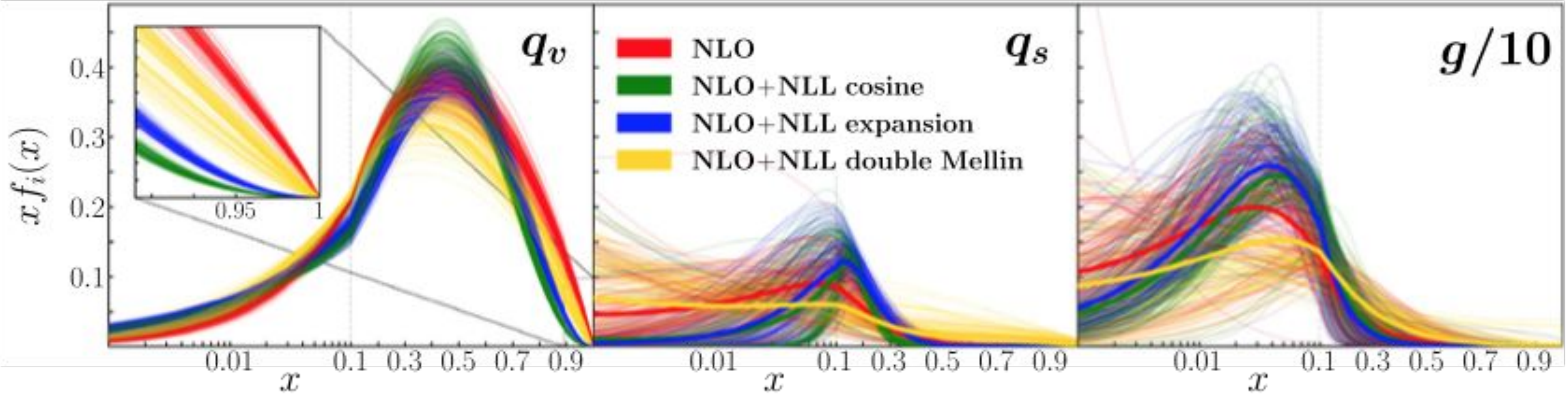

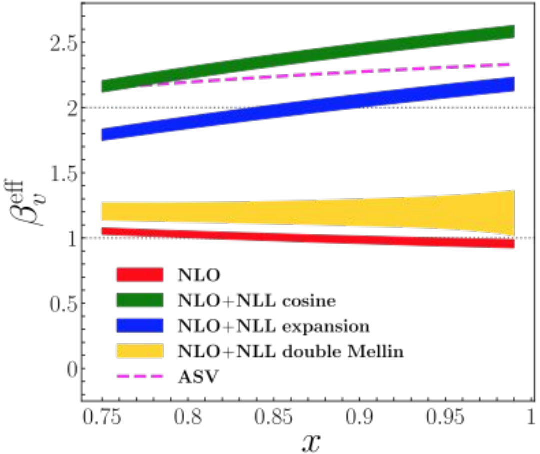

Resummation method	$\langle x \rangle_v$	$\langle x \rangle_s$	$\langle x \rangle_g$
NLO	0.53(2)	0.14(4)	0.34(6)
NLO + NLL cosine	0.47(2)	0.14(5)	0.39(6)
NLO + NLL expansion	0.46(2)	0.16(5)	0.38(6)
NLO + NLL double Mellin	0.46(3)	0.15(7)	0.40(5)

Measurement of Tagged Deep Inelastic Scattering (TDIS)

C.Keppel (Contact person)

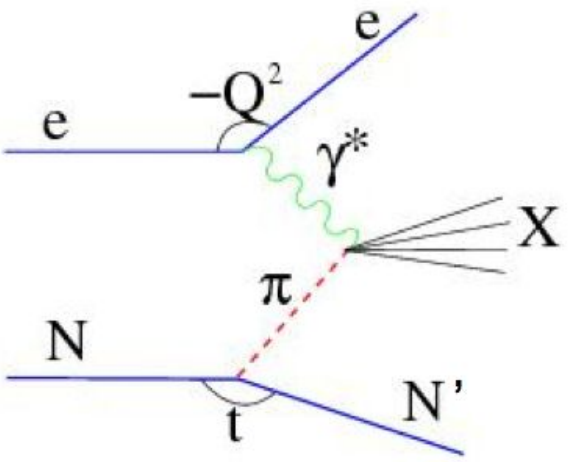

$$e + p(or\ n) \rightarrow e' + p + X$$

$$e + D \rightarrow e' + p + p + X$$

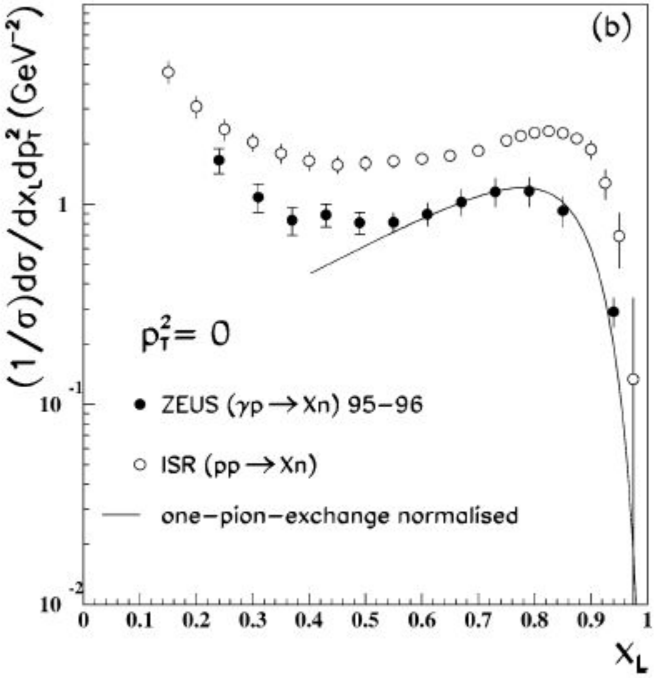

Leading neutron production in e^+p collisions at HERA

ZEUS Collaboration, NPB 637 (2002) 3–56

Hadron Physics and QCD Phenomenology with 12 GeV Upgrade of Jefferson Laboratory

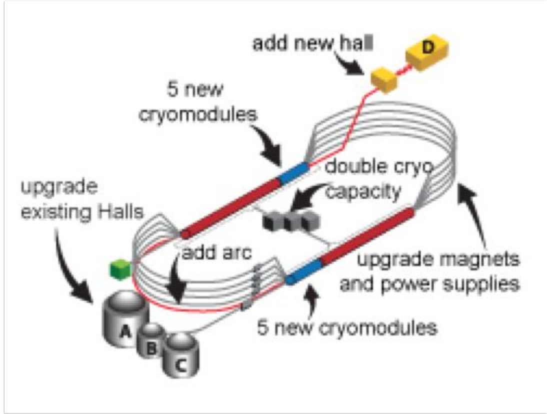

JLab Hall A TDIS Experiment

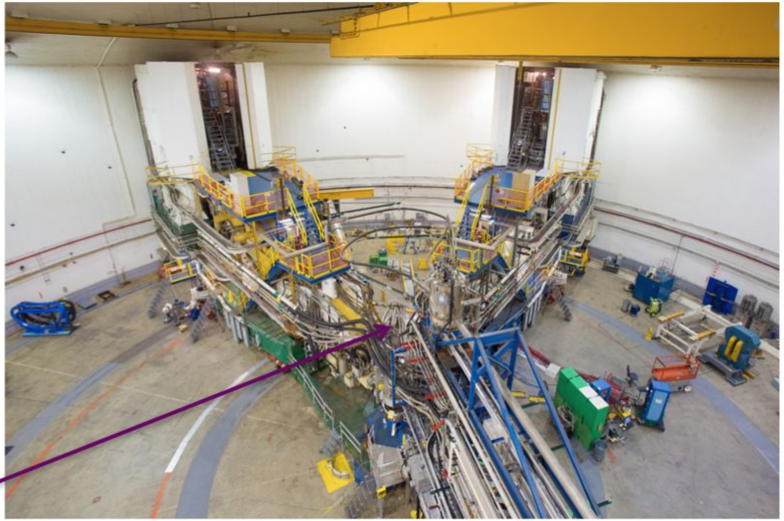

proton tag detection in GEM-based mTPC at pivot

Hall A with SBS:

✓High luminosity, 50 μAmp, $\mathcal{L} = 3\text{x}10^{36}/\text{cm}^2\ \text{s}$

✓Large acceptance ~70 msr

Important for small cross sections

e- beam

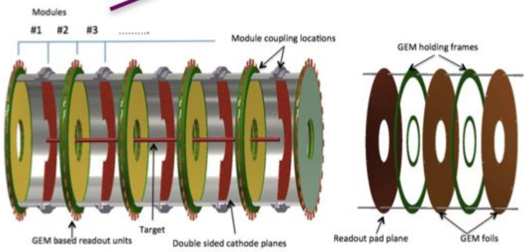

mTPC inside superconducting solenoid

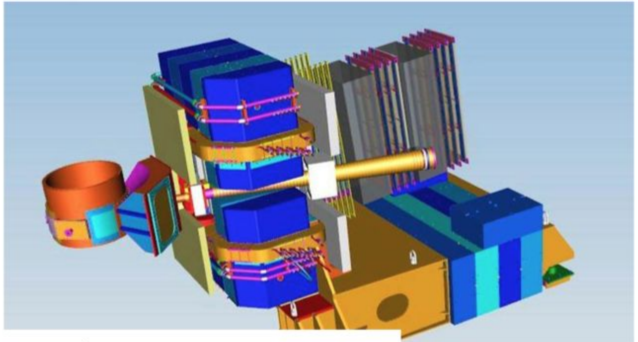

Scattered electron detection in new Super Bigbite Spectrometer (SBS) – DOE project complete

Jianwei Qiu
Jefferson Lab, Theory Center

Major Facilities and experiments:

- Argonne Tandem Linac Accelerator System (**ATLAS**)
- Facility for Rare Isotope Beams (**FRIB**)
- Continuous Electron Beam Accelerator Facility (**CEBAF**)
- Relativistic Heavy Ion Collider (**RHIC**)
- Electron Ion Collider (**EIC**)

Energy Scale probed: ~ 20 MeV → 200 MeV → > 2 GeV

Color Confinement — Asymptotic freedom

Distance scale probed: 10 fm, 1 fm, 0.1 fm — Q (GeV)

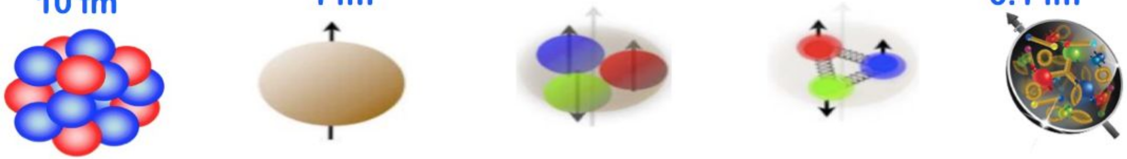

Physics topics:

- Nuclear reactions
- Fission and nucleosynthesis
- Properties of nuclei
- Nuclear structure
- Microscopic models

- Hadron spectra
- Exotic states of QCD
- Neutrino and electron interactions in nuclei and dense matter

- Nuclear tomography at femtometer scale (New)
- Properties of quark-gluon plasma

2022 FOA physics topics in the context of NP program

Major Facilities and experiments:

Argonne Tandem Linac Accelerator System (**ATLAS**)

Facility for Rare Isotope Beams (**FRIB**)

Continuous Electron Beam Accelerator Facility (**CEBAF**)

Relativistic Heavy Ion Collider (**RHIC**)

Electron Ion Collider (**EIC**)

Energy Scale probed

Distance scale probed

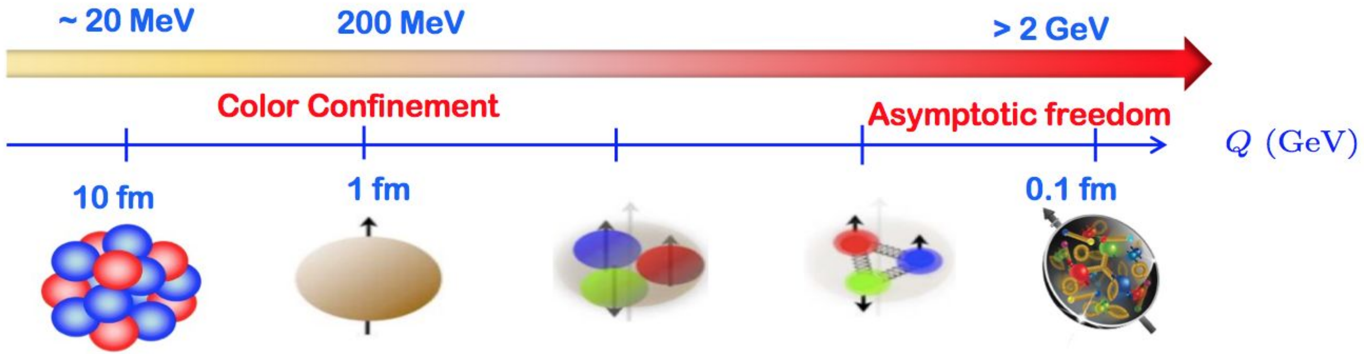

Physics topics:

- Nuclear reactions
- Fission and nucleosynthesis
- Properties of nuclei
- Nuclear structure
- Microscopic models

- Hadron spectra
- Exotic states of QCD
- Neutrino and electron interactions in nuclei and dense matter

- Nuclear tomography at femtometer scale (New)
- Properties of quark-gluon plasma

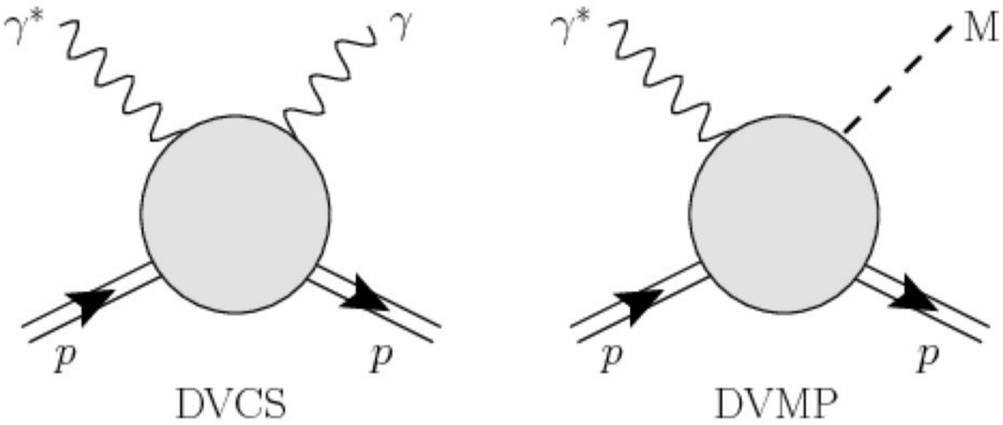

Q^2 >> M^2, |t|,..

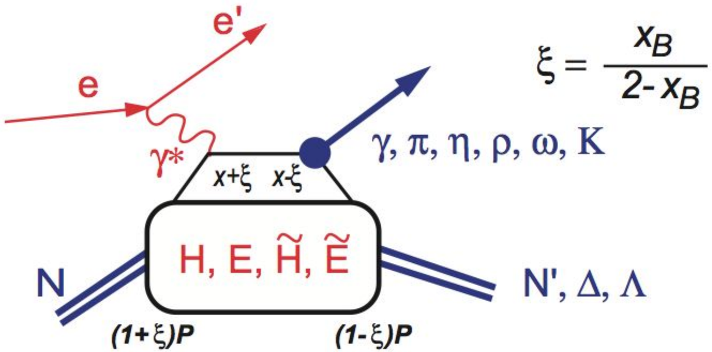

H, E - unpolarized, $\widetilde{H}$, $\widetilde{E}$ - polarized GPD

The GPDs Define Nucleon Structure

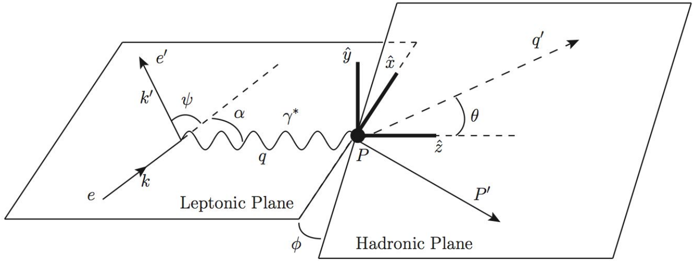

5-Fold Differential Cross Section

$$\frac{d\sigma_v}{d\Omega} = \frac{d\sigma_T}{d\Omega} + \varepsilon \frac{d\sigma_L}{d\Omega} + \sqrt{2\varepsilon(1+\varepsilon)}\frac{d\sigma_{LT}}{d\Omega}\cos\phi + \varepsilon \frac{d\sigma_{TT}}{d\Omega}\cos 2\phi + h\sqrt{2\varepsilon(1-\varepsilon)}\frac{d\sigma_{LT'}}{d\Omega}\sin\phi$$

https://maid.kph.uni-mainz.de/maid2007/cross.html

Mainz analysis interactive database (MAID)

$$J^\mu_{PS} = F_{PS}\epsilon^{\mu\nu\alpha\beta} q_\nu \bar{P}_\alpha \Delta_\beta$$

$$\begin{aligned}\mathcal{H}_{\mu\nu} &= J^\dagger_\mu J_\nu \\ &= |F_{PS}|^2 \epsilon_{\mu\alpha\beta\gamma}\epsilon_{\nu\alpha'\beta'\gamma'} q^\alpha \bar{P}^\beta \Delta^\gamma q^{\alpha'} \bar{P}^{\beta'} \Delta^{\gamma'} \\ &= \mathcal{H}_{\nu\mu}\end{aligned}$$

$$\epsilon^{\mu\nu\alpha\beta} k_\alpha k'_\beta \mathcal{H}_{\mu\nu} = 0$$

$$\frac{d\sigma^{PS}_{\lambda=+1} - d\sigma^{PS}_{\lambda=-1}}{d\sigma^{PS}_{\lambda=+1} + d\sigma^{PS}_{\lambda=-1}} = 0$$

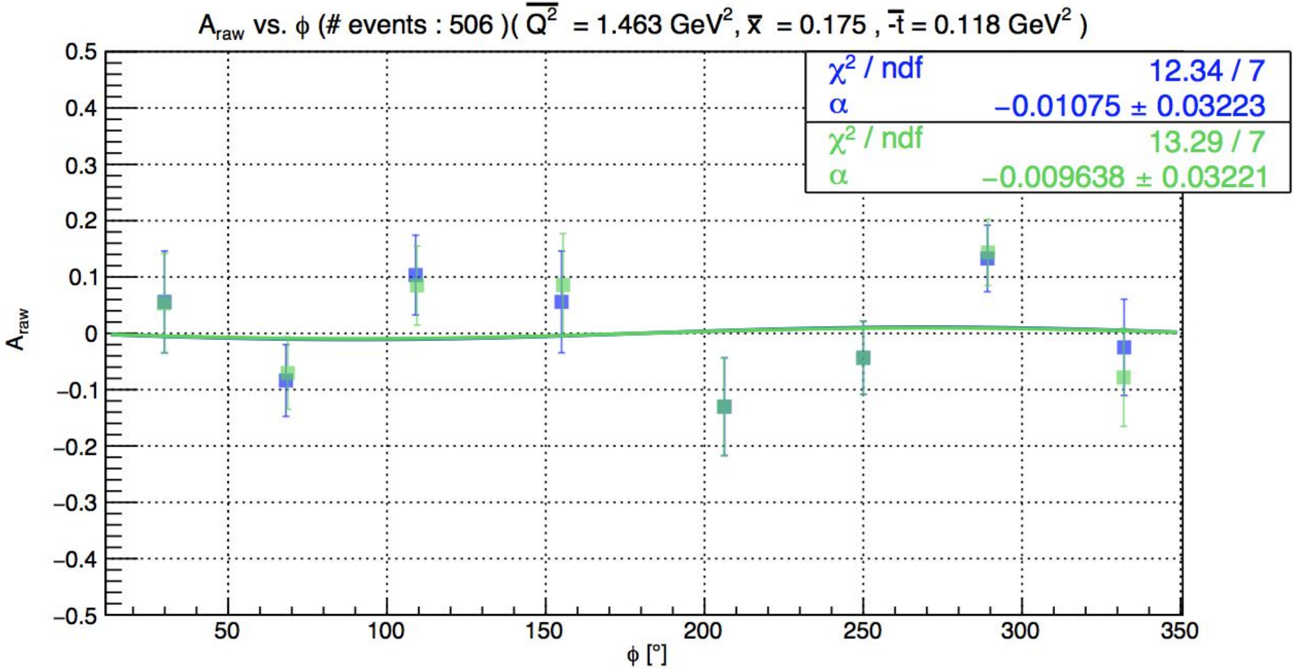

$$A_{LU}(\phi) = A_{LU}^{90^\circ} \sin\phi$$

$$A_{LU}^{90^\circ} = -1.08 \pm 3.22\,(\text{stat.}) \pm 2.83\,(\text{sys.})\,\%$$

4-26-2019

Beam-Spin Asymmetry of Exclusive Coherent Electroproduction of the π0 Off 4He

Frank Thanh Cao
University of Connecticut - Storrs, franktcao@gmail.com

Beam-Spin Asymmetry of Exclusive Coherent Electroproduction of the π^0 Off ^{4}He

Frank Thanh Cao, Ph.D.

University of Connecticut, 2019

To understand the partonic structure of nucleons in nuclei, extracting the beam spin asymmetry (BSA) from exclusive processes is an important measurement to get at the so-called Generalized Parton Distributions (GPDs) that describe the partons behavior inside the nucleon. In particular, BSA in Deeply Virtual Meson Production (DVMP) can offer valuable constraints on the transverse GPDs which are not accessible through Deeply Virtual Compton Scattering (DVCS).

……

This benchmark measurement is in agreement with symmetry arguments presented in a recent theoretical formulation [2] that offers a framework complementary to that of the GPDs and gives confidence in the assumptions made for future studies of exclusive nuclear processes.

PHYSICAL REVIEW D **99,** 116008 (2019)

Beam spin asymmetry in the electroproduction of a pseudoscalar meson or a scalar meson off the scalar target

Chueng-Ryong Ji,[1] Ho-Meoyng Choi,[2] Andrew Lundeen,[1] and Bernard L. G. Bakker[3]
[1]*Department of Physics, North Carolina State University, Raleigh, North Carolina 27695-8202, USA*
[2]*Department of Physics, Teachers College, Kyungpook National University, Daegu 41566, Korea*
[3]*Faculteit der Bètawetenschappen, Vrije Universiteit, Amsterdam, Netherlands*

(Received 25 February 2019; published 12 June 2019)

We discuss the electroproduction of a pseudoscalar (0^{-+}) meson or a scalar (0^{++}) meson off the scalar target. The most general formulation of the differential cross section for the 0^{-+} or 0^{++} meson process involves only one or two hadronic form factors, respectively, on a scalar target. The Rosenbluth-type separation of the differential cross section provides the explicit relation between the hadronic form factors and the different parts of the differential cross section in a completely model-independent manner. The absence of the beam spin asymmetry for the pseudoscalar meson production provides a benchmark for the experimental data analysis. The measurement of the beam spin asymmetry for the scalar meson production may also provide a unique opportunity not only to explore the imaginary part of the hadronic amplitude in the general formulation but also to examine the significance of the chiral-odd generalized parton distribution (GPD) contribution in the leading-twist GPD formulation.

Better Work in Forward Direction

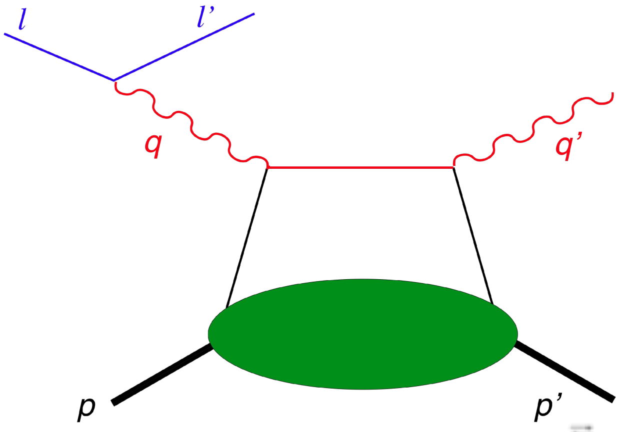

GPD

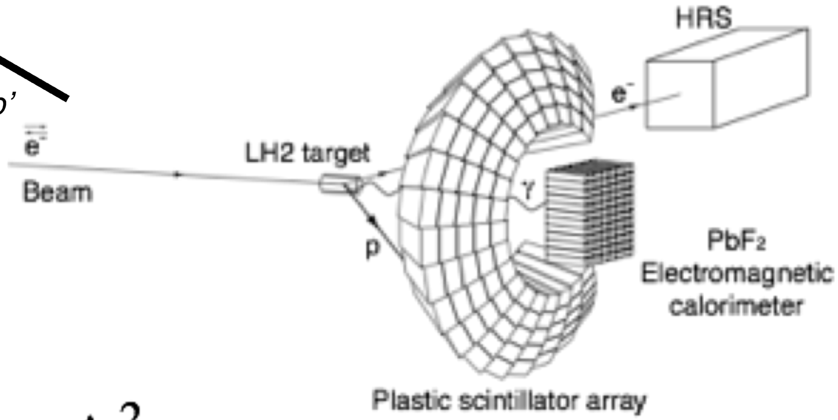

LFD

$$t = \Delta^2 = -\frac{\zeta^2 M^2 + \Delta_\perp^2}{1-\zeta}; \Delta^+ (\equiv \Delta^0 + \Delta^3) = \zeta P^+; \Delta_\perp^2 > \Delta_{\perp\min}^2 \neq 0$$

PHYSICAL REVIEW D **105,** 096014 (2022)

Analysis of virtual meson production in a (1 + 1)-dimensional scalar field model

Yongwoo Choi,[1,*] Ho-Meoyng Choi,[2,†] Chueng-Ryong Ji,[3,‡] and Yongseok Oh[1,4,§]

[1]*Department of Physics, Kyungpook National University, Daegu 41566, Korea*
[2]*Department of Physics Education, Teachers College, Kyungpook National University, Daegu 41566, Korea*
[3]*Department of Physics, North Carolina State University, Raleigh, North Carolina 27695-8202, USA*
[4]*Asia Pacific Center for Theoretical Physics, Pohang, Gyeongbuk 37673, Korea*

(Received 10 December 2021; accepted 30 March 2022; published 17 May 2022)

PHYSICAL REVIEW D **103,** 076002 (2021)

Light-front dynamic analysis of the longitudinal charge density using the solvable scalar field model in (1 + 1) dimensions

Yongwoo Choi,[1] Ho-Meoyng Choi,[2,*] Chueng-Ryong Ji,[3,†] and Yongseok Oh[1,4,‡]

Scalar Field Model Simulation of VMP in Forward Direction

$$\text{“}\gamma^* + {}^4\text{He} \rightarrow f_0(980) + {}^4\text{He}\text{”}$$

$$\mathcal{M}^{\mu(1+1)}_{\text{tot}} = [(\Delta \cdot q)q^\mu - q^2\Delta^\mu]\mathcal{F}$$

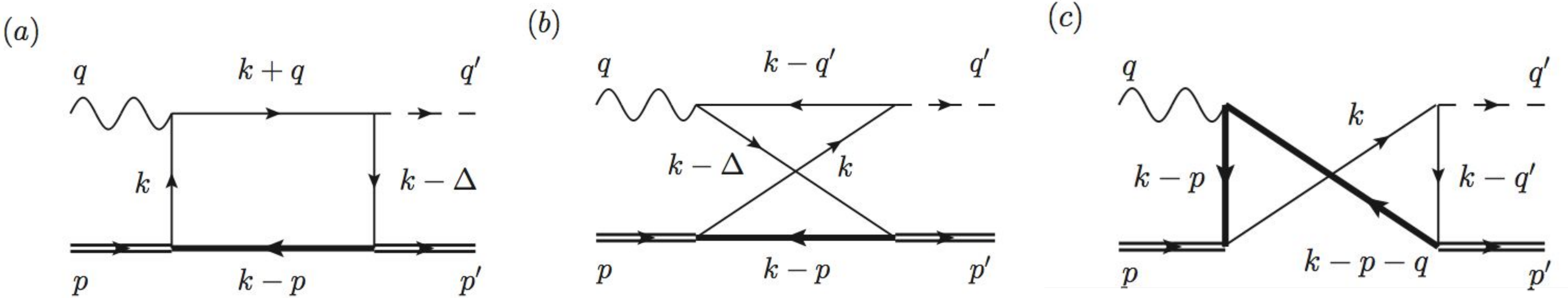

Two more amplitudes for the charged target, but not for the neutral target

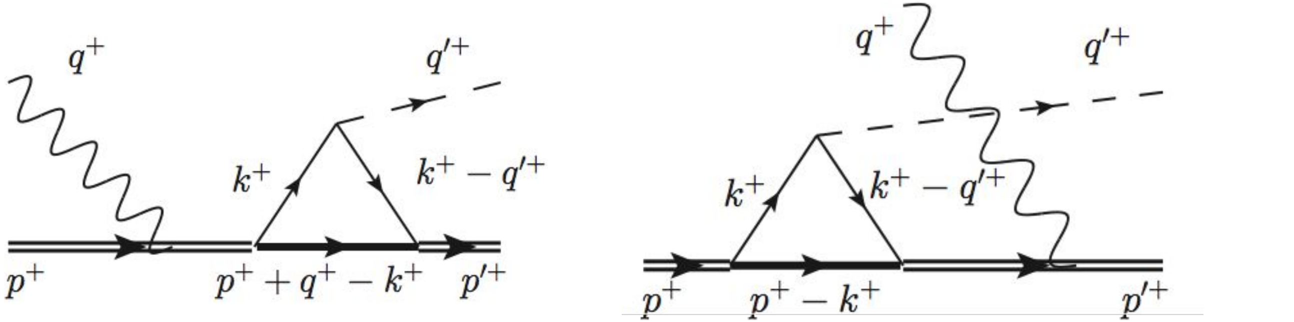

Light-Front Time-Ordered Amplitudes

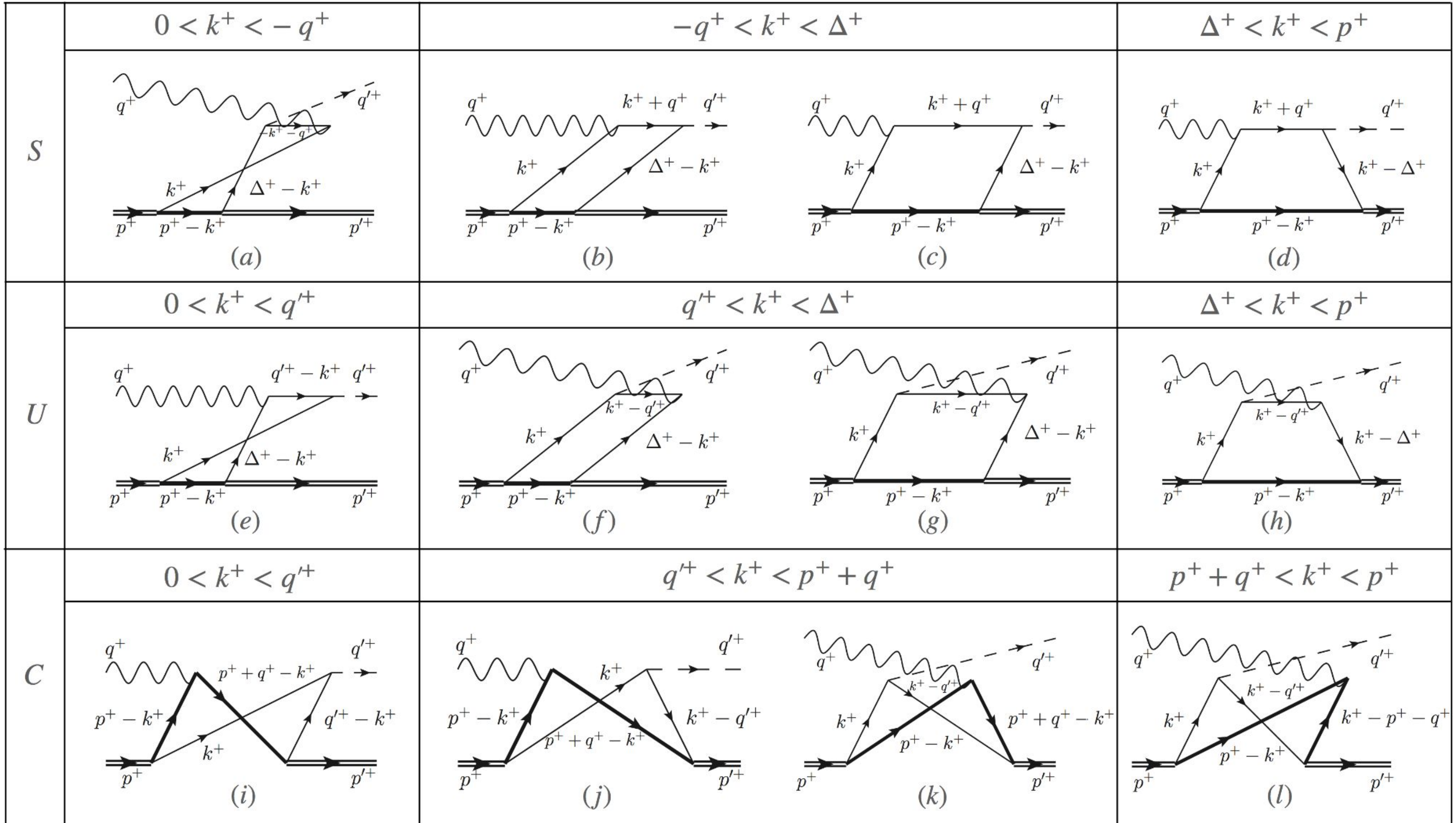

$t = t_{\rm th} \simeq -0.7593\,{\rm GeV}^2$

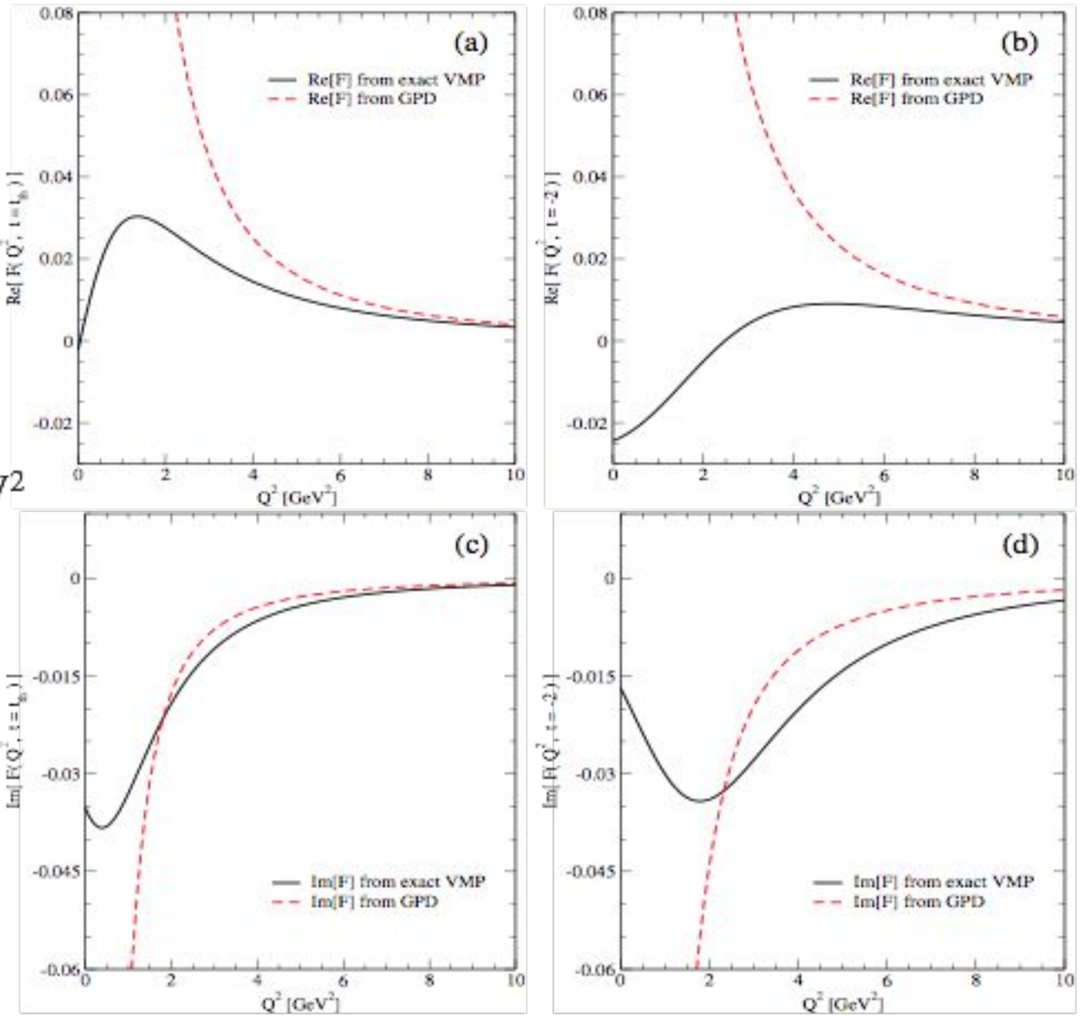

$t = -2\,{\rm GeV}^2$

$-t/Q^2 \lesssim 0.1$

Dirac's Proposition for Relativistic Dynamics

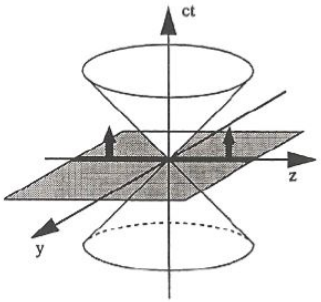

The instant form

1949

Equal t		Equal τ
p^0	$\leftrightarrow$	$p^- = p^0 - p^3$
(p^1, p^2)	$\leftrightarrow$	$\vec{p}_\perp$
p^3	$\leftrightarrow$	$p^+ = p^0 + p^3$

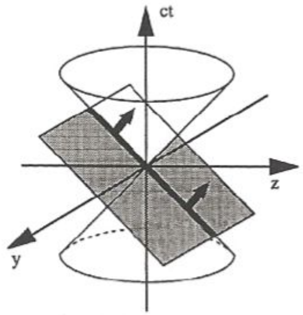

The front form

Energy-Momentum Dispersion Relations

$$p^0 = \sqrt{\vec{p}^{\,2} + m^2} \qquad\qquad p^- = \frac{\vec{p}_\perp^{\,2} + m^2}{p^+}$$

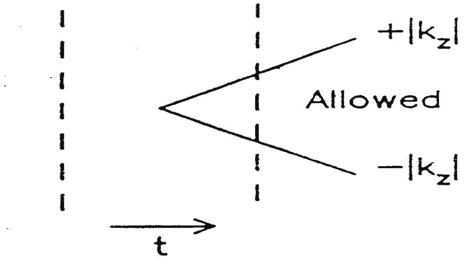

(a)

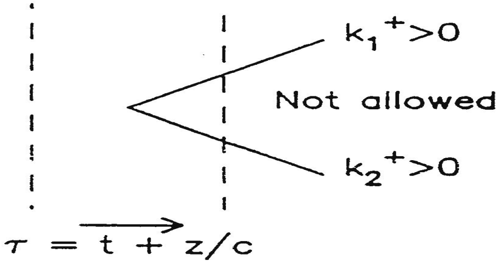

(b)

Except zero-modes

$k_1^+ = k_2^+ = 0$

IFD

Instant Form Dynamics

LFD

Light-Front Dynamics

Interpolation between IFD and LFD

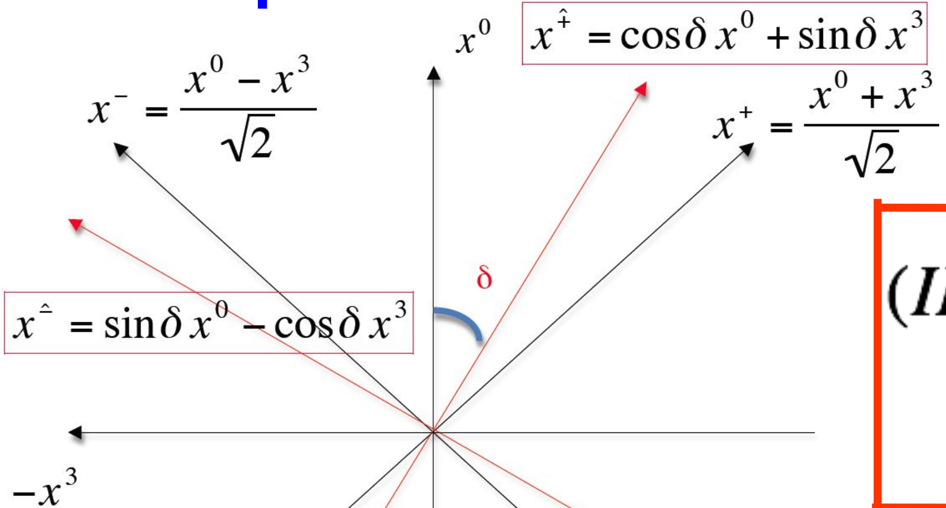

$$(IFD) \quad 0 \le \delta \le \frac{\pi}{4} \quad (LFD)$$

$$1 \ge \quad C \equiv \cos(2\delta) \quad \ge 0$$

K. Hornbostel, PRD45, 3781 (1992) – RQFT
C.Ji and S.Rey, PRD53,5815(1996) – Chiral Anomaly
C.Ji and C. Mitchell, PRD64,085013 (2001) – Poincare Algebra
C.Ji and A. Suzuki, PRD87,065015 (2013) – Scattering Amps
C.Ji, Z. Li and A. Suzuki, PRD91, 065020 (2015) – EM Gauges
Z.Li, M. An and C.Ji, PRD92, 105014 (2015) – Spinors
C.Ji, Z.Li, B.Ma and A.Suzuki, PRD98, 036017(2018) – QED
B.Ma and C.Ji, PRD194,036004(2021) – QCD_{1+1}

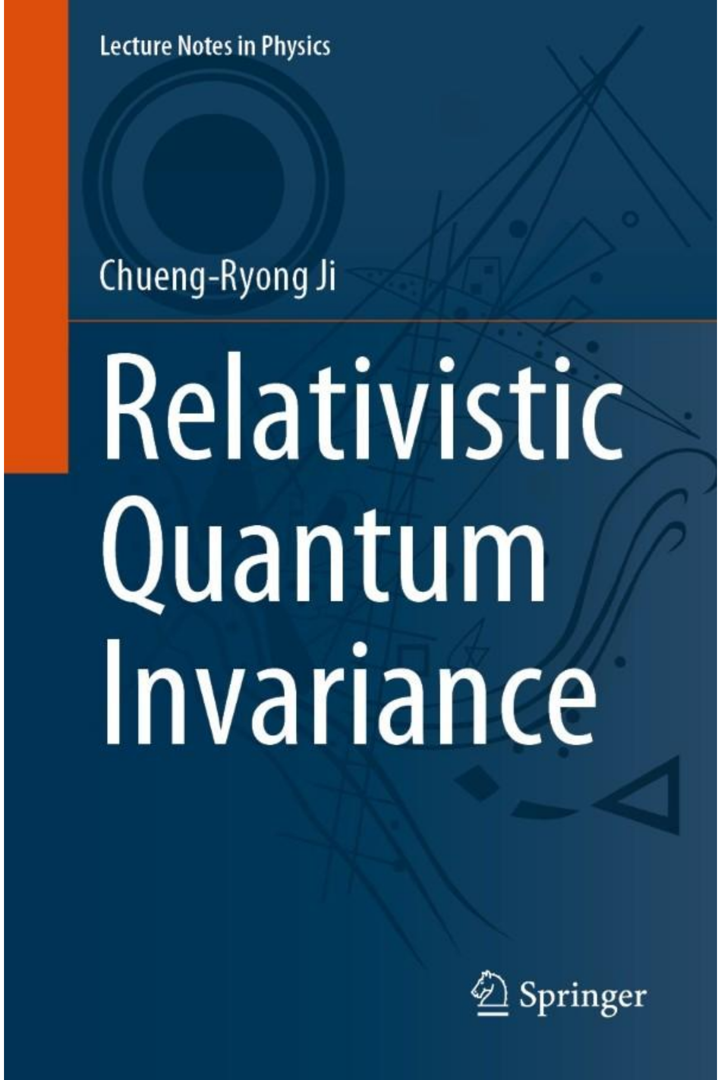

Interpolating instant form dynamics and light-front dynamics

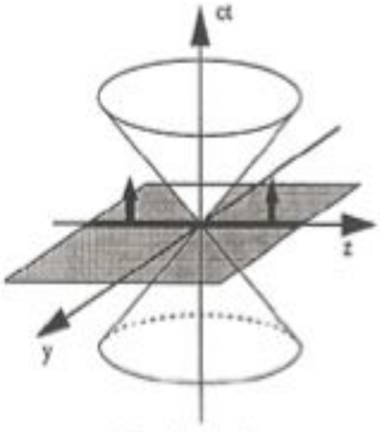

The instant form

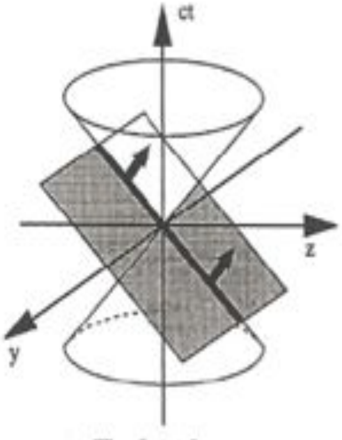

The front form

Large N_c QCD in 1+1 dim. ('tHooft Model)

$$\mathcal{L} = -\frac{1}{4} F^a_{\hat{\mu}\hat{\nu}} F^{\hat{\mu}\hat{\nu}a} + \bar{\psi}(i\gamma^{\hat{\mu}} D_{\hat{\mu}} - m)\psi$$

$$D_{\hat{\mu}} = \partial_{\hat{\mu}} - igA^a_{\hat{\mu}} t_a$$

$$F^a_{\hat{\mu}\hat{\nu}} = \partial_{\hat{\mu}} A^a_{\hat{\nu}} - \partial_{\hat{\nu}} A^a_{\hat{\mu}} + g f^{abc} A^b_{\hat{\mu}} A^c_{\hat{\nu}}$$

'tHooft Coupling $\lambda = \frac{g^2 (N_c - 1/N_c)}{4\pi}$ and mass m

$$g \to 0, N_C \to \infty; \lambda \to finite$$

Interpolating Axial Gauge

$$A^a_{\hat{-}} = 0$$

$$A^a_1 = 0 \qquad\qquad A^+_a = 0$$

$$\mathcal{L} = \frac{1}{2}(\partial_{\hat{-}} A^a_{\hat{+}})^2 + \bar{\psi}(i\gamma^{\hat{+}} D_{\hat{+}} + i\gamma^{\hat{-}}\partial_{\hat{-}} - m)\psi$$

Mass Gap Equation

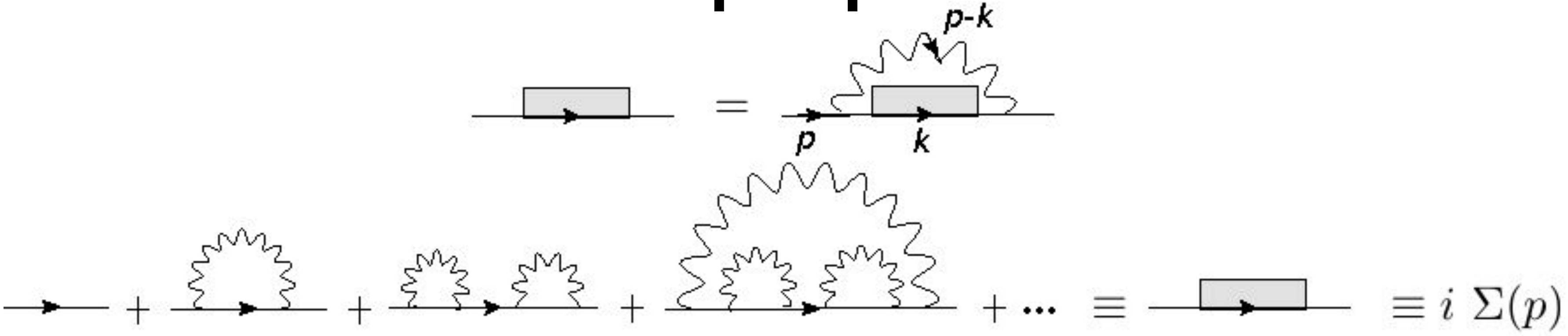

$$\Sigma(p_{\hat{-}}) = i\frac{\lambda}{2\pi}\int \frac{dk_{\hat{-}}dk_{\hat{+}}}{(p_{\hat{-}} - k_{\hat{-}})^2}\gamma^{\hat{+}}\frac{1}{\not{k} - m - \Sigma(k_{\hat{-}}) + i\epsilon}\gamma^{\hat{+}}$$

Fermion Propagator

Free Propagator

$$S_f(p) = \frac{1}{\not{p} - m + i\varepsilon}$$

$$\Sigma(p) = \Sigma_s(p) + \Sigma_v(p)\not{p}$$

Interacting Propagator

$$S(p) = \frac{1}{\not{p} - m - \Sigma(p) + i\varepsilon}$$

$$= \frac{F(p)}{\not{p} - M(p) + i\varepsilon}$$

$$F(p) = \left(1 - \Sigma_v(p)\right)^{-1}$$ "Wave function renormalization factor"

$$M(p) = \frac{m + \Sigma_s(p)}{1 - \Sigma_v(p)}$$ "Renormalized fermion mass function"

Energy-Momentum Dispersion Relation

Free particle | **Interacting particle**

$$E = \sqrt{p_z^2 + m^2}$$

$$\theta_f = \tan^{-1}(p_z / m)$$

$$\beta = p_z / E$$

$$= \sin\theta_f$$

$$= \tanh\eta$$

$$\frac{F(p'_-)E(p'_-)}{\sqrt{C}} = \sqrt{p'^2_- + M(p'_-)^2} \equiv \tilde{E}(p'_-)$$

$$\theta(p'_-) = \theta_f(p'_-) + 2\zeta(p'_-)$$

$$\begin{pmatrix} b^i(p'_-) \\ d^{+i}(p'_-) \end{pmatrix} = \begin{pmatrix} \cos\zeta(p'_-) & -\sin\zeta(p'_-) \\ \sin\zeta(p'_-) & \cos\zeta(p'_-) \end{pmatrix} \begin{pmatrix} b^i_f(p'_-) \\ d^{+i}_f(p'_-) \end{pmatrix}$$

$$b^i_f|0\rangle = 0,\ d^i_f|0\rangle = 0 \quad \text{vs.} \quad b^i|\Omega\rangle = 0,\ d^i|\Omega\rangle = 0$$

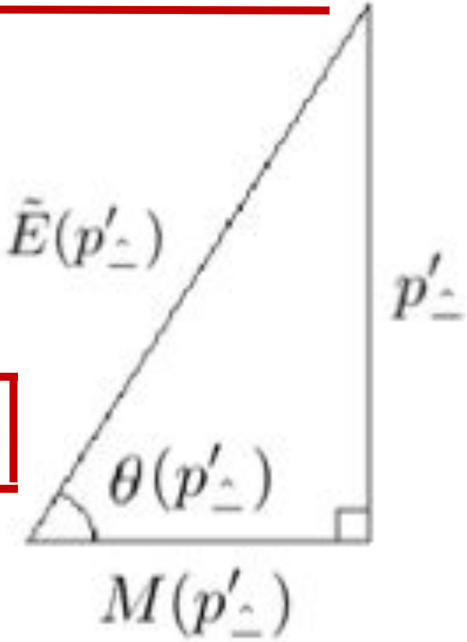

Interpolation

$$(E, p_z) \Rightarrow (p^+/\sqrt{C},\ p_- / \sqrt{C} \equiv p'_-)$$

Mass Gap Equation in Scaled Variables

$$\bar{p}'_{\perp} = \frac{\bar{p}_{\perp}}{\sqrt{\mathbb{C}}},\ \bar{E}' = \frac{\bar{E}}{\sqrt{\mathbb{C}}}, \bar{p}_{\perp} = \frac{p_{\perp}}{\sqrt{2\lambda}},\ \bar{E} = \frac{E}{\sqrt{2\lambda}}, \bar{m} = \frac{m}{\sqrt{2\lambda}}$$

$$\bar{p}'_{\perp} \cos\theta(\bar{p}'_{\perp}) - \bar{m}\sin\theta(\bar{p}'_{\perp}) = \frac{1}{4}\int \frac{d\bar{k}'_{\perp}}{(\bar{p}'_{\perp} - \bar{k}'_{\perp})^2} \sin\Big(\theta(\bar{p}'_{\perp}) - \theta(\bar{k}'_{\perp})\Big)$$

$$\bar{E}'(\bar{p}'_{\perp}) = \bar{p}'_{\perp}\sin\theta(\bar{p}'_{\perp}) + \bar{m}\cos\theta(\bar{p}'_{\perp}) + \frac{1}{4}\int \frac{d\bar{k}'_{\perp}}{(\bar{p}'_{\perp} - \bar{k}'_{\perp})^2} \cos\Big(\theta(\bar{p}'_{\perp}) - \theta(\bar{k}'_{\perp})\Big)$$

$$\frac{p_{\perp}}{\mathbb{C}}\cos\theta(p_{\perp}) - \frac{m}{\sqrt{\mathbb{C}}}\sin\theta(p_{\perp}) = \frac{\lambda}{2}\int \frac{dk_{\perp}}{(p_{\perp} - k_{\perp})^2}\sin\left(\theta(p_{\perp}) - \theta(k_{\perp})\right)$$

$$E(p_{\perp}) = p_{\perp}\sin\theta(p_{\perp}) + \sqrt{\mathbb{C}}m\cos\theta(p_{\perp}) + \frac{\mathbb{C}\lambda}{2}\int \frac{dk_{\perp}}{(p_{\perp} - k_{\perp})^2}\cos\left(\theta(p_{\perp}) - \theta(k_{\perp})\right)$$

Mass Gap Solutions

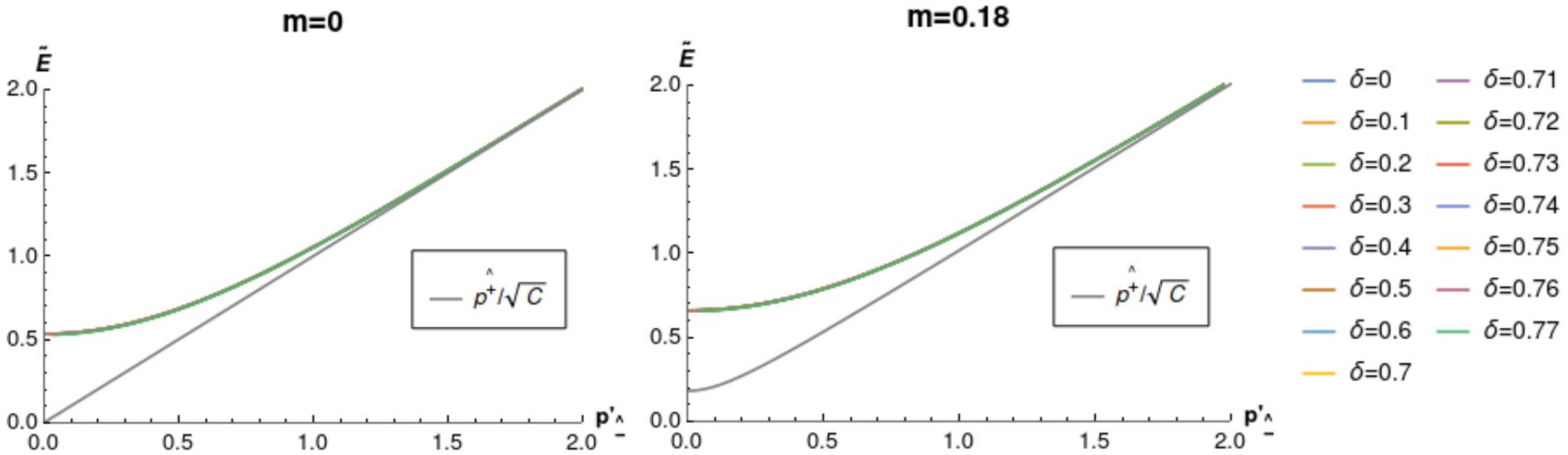

$$\tilde{E}(0) = \frac{F(0)E(0)}{\sqrt{\mathbb{C}}} = M(0)$$

m	0	0.045	0.18	0.749	1.00	2.11	4.23
$M(0)$	0.532778	0.563644	0.659112	1.10105	1.31167	2.30969	4.34358
$F(0)$	−0.495173	−0.584175	−0.987673	4.11079	2.17976	1.22134	1.05526

$$m \lesssim 0.56$$

BOUND-STATE EQUATION

$$\Gamma(r,p) = \frac{i\lambda}{2\pi}\int \frac{dk_{\hat{-}}\, dk_{\hat{+}}}{(p_{\hat{-}} - k_{\hat{-}})^2} S(p)\gamma^{\hat{+}}\Gamma(r,k)\gamma^{\hat{+}} S(p-r)$$

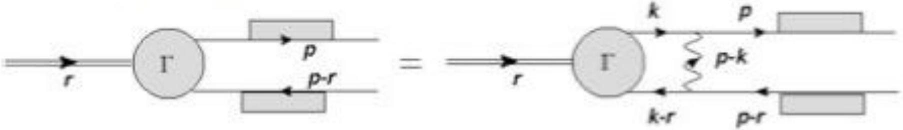

$$\left[-r_{\hat{+}} + \frac{-\mathbb{S}p_{\hat{-}} + E(p_{\hat{-}})}{\mathbb{C}} + \frac{\mathbb{S}(p_{\hat{-}} - r_{\hat{-}}) + E(p_{\hat{-}} - r_{\hat{-}})}{\mathbb{C}}\right]\hat{\phi}_+(r_{\hat{-}}, p_{\hat{-}})$$
$$= \lambda \fint \frac{dk_{\hat{-}}}{(p_{\hat{-}} - k_{\hat{-}})^2}\left[C(p_{\hat{-}}, k_{\hat{-}}, r_{\hat{-}})\hat{\phi}_+(r_{\hat{-}}, k_{\hat{-}}) - S(p_{\hat{-}}, k_{\hat{-}}, r_{\hat{-}})\hat{\phi}_-(r_{\hat{-}}, k_{\hat{-}})\right],$$

$$\left[r_{\hat{+}} + \frac{-\mathbb{S}(p_{\hat{-}} - r_{\hat{-}}) + E(p_{\hat{-}} - r_{\hat{-}})}{\mathbb{C}} + \frac{\mathbb{S}p_{\hat{-}} + E(p_{\hat{-}})}{\mathbb{C}}\right]\hat{\phi}_-(r_{\hat{-}}, p_{\hat{-}})$$
$$= \lambda \fint \frac{dk_{\hat{-}}}{(p_{\hat{-}} - k_{\hat{-}})^2}\left[C(p_{\hat{-}}, k_{\hat{-}}, r_{\hat{-}})\hat{\phi}_-(r_{\hat{-}}, k_{\hat{-}}) - S(p_{\hat{-}}, k_{\hat{-}}, r_{\hat{-}})\hat{\phi}_+(r_{\hat{-}}, k_{\hat{-}})\right].$$

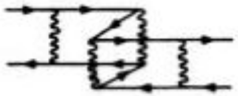

LFD $$\left[\mathcal{M}^2 - \frac{m^2 - 2\lambda}{x} - \frac{m^2 - 2\lambda}{1-x}\right]\phi(x) = -2\lambda \fint_0^1 \frac{dy}{(x-y)^2}\phi(y)$$

Meson Spectroscopy

- G.‘tHooft, NPB75, 461(74) - LFD

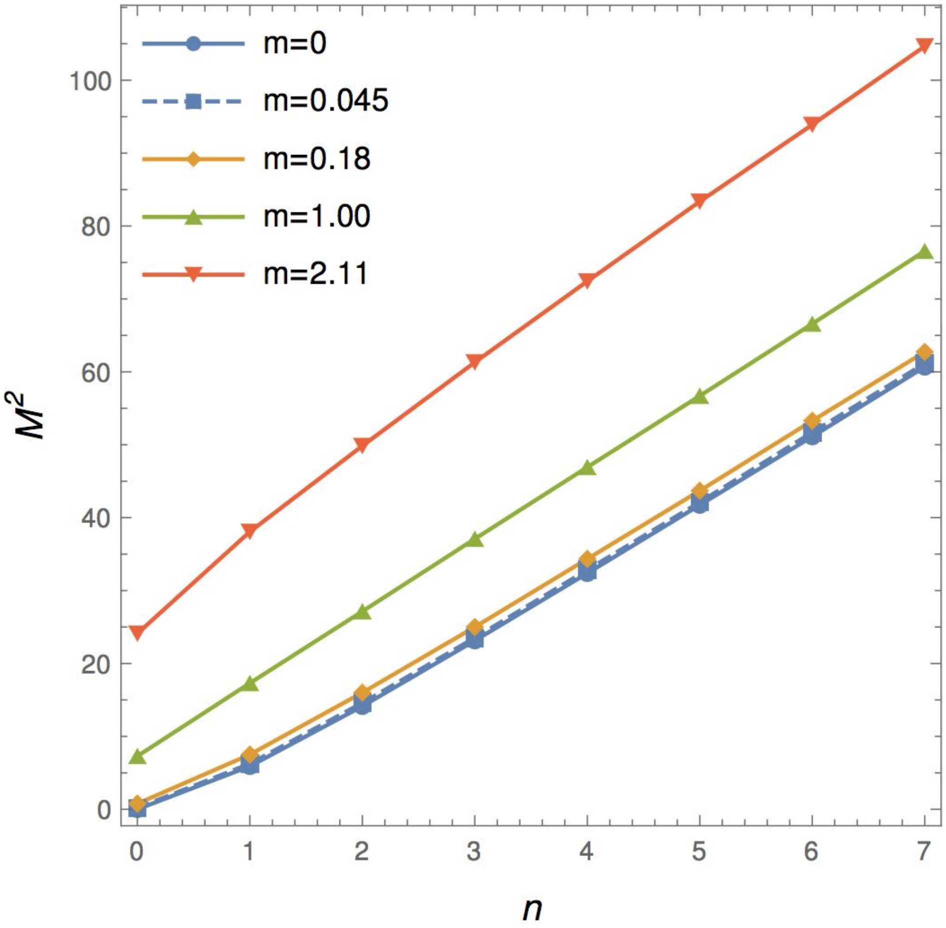

- M.Li, et al., JPG13, 915(87) - IFD (rest frame)
- Y. Jia, et al., JHEP11, 151(‘17) - IFD (moving frame)

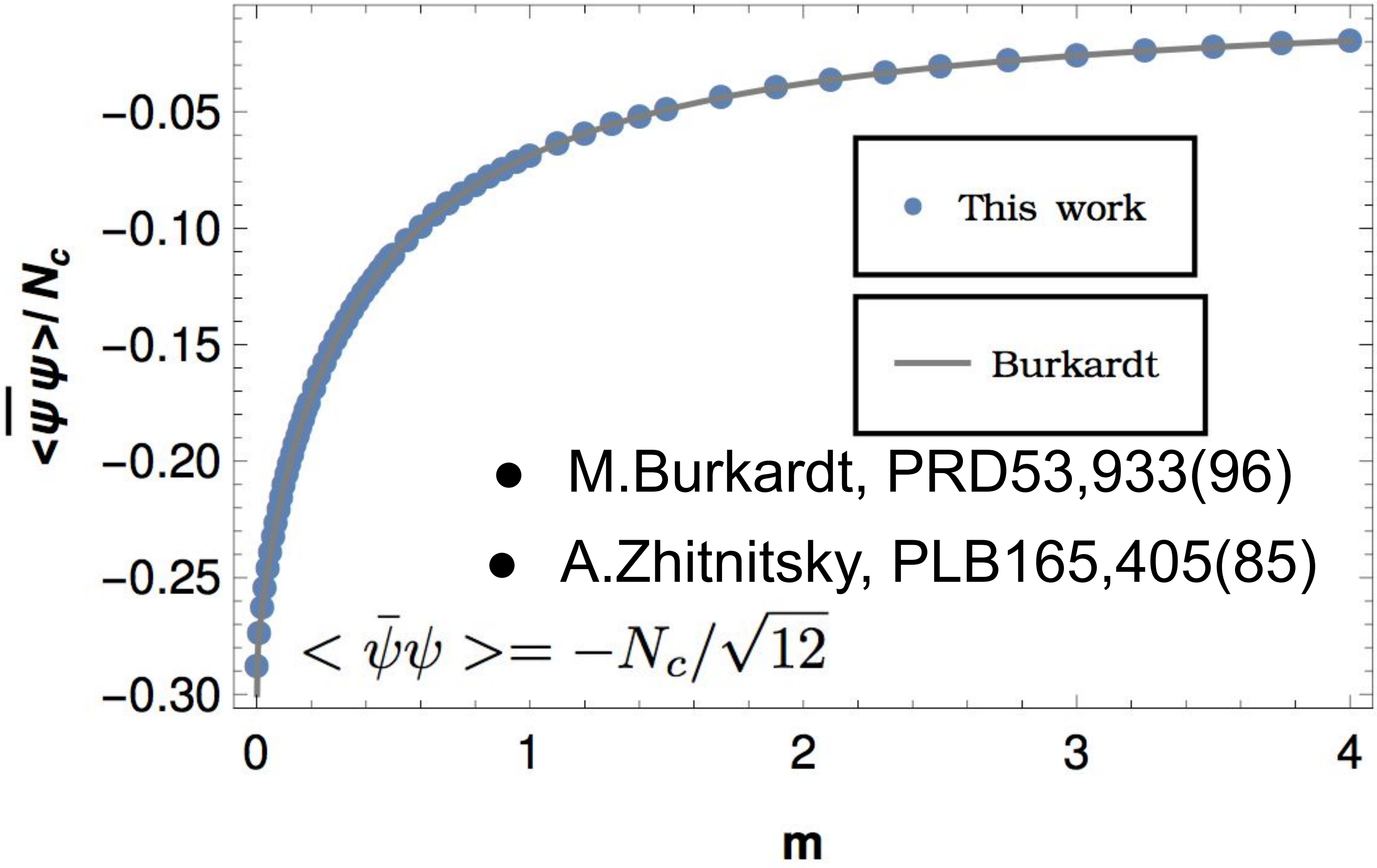

$\overline{\psi}\psi$/N_c
m
This work
Burkardt
$< \bar{\psi}\psi >= -N_c/\sqrt{12}$
−0.05
−0.10
−0.15
−0.20
−0.25
−0.30
0
1
2
3
4
• M.Burkardt, PRD53,933(96)
• A.Zhitnitsky, PLB165,405(85)

Gell-Mann - Oaks - Renner Relation

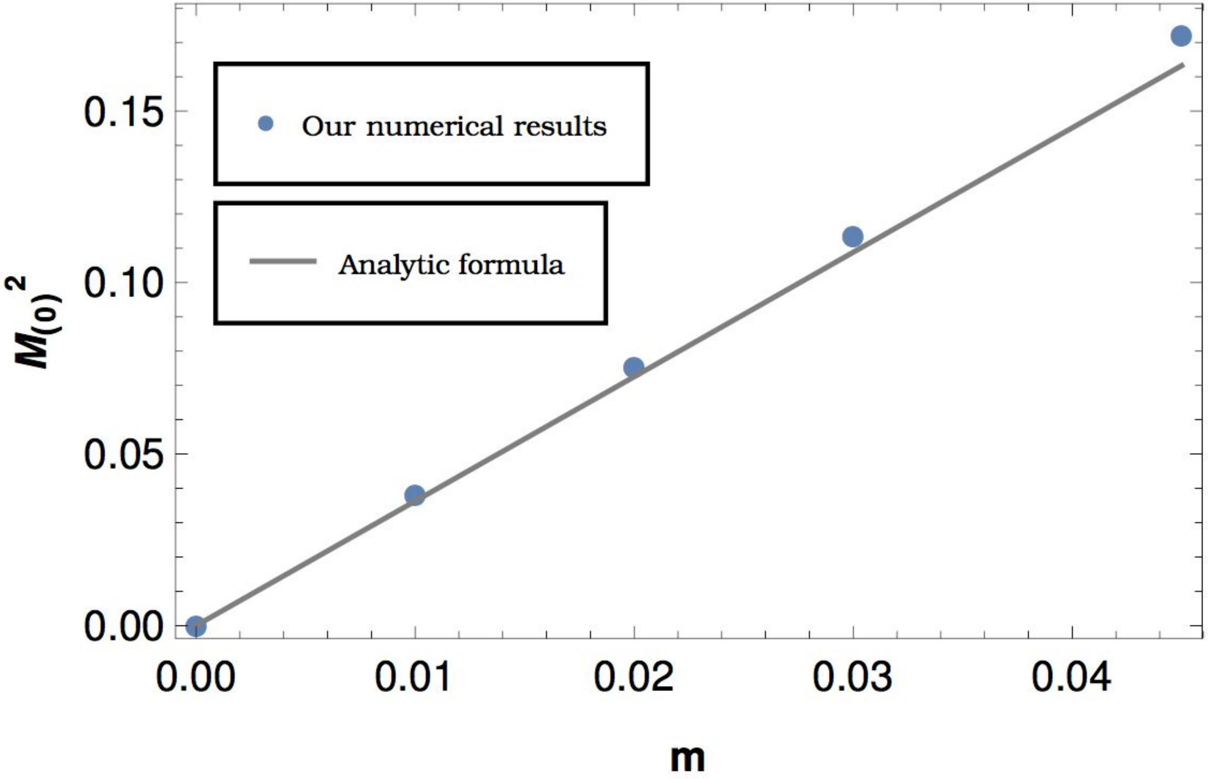

$$\mathcal{M}_\pi^2 = -\frac{4m < \bar{\psi}\psi >}{f_\pi^2} = \sqrt{\frac{8\pi^2 m^2 \lambda}{3}}$$

$$f_\pi = \sqrt{N_c/\pi}$$

Effective Constituent Quark Model for Low Q^2

$$|Meson\rangle = \psi_{q\bar{q}}|q\bar{q}\rangle + \psi_{q\bar{q}g}|q\bar{q}g\rangle + \dots$$
$$\approx \Psi_{Q\bar{Q}}|Q\bar{Q}\rangle,$$

where

$$|Q\rangle = \psi_q^Q|q\rangle + \psi_{qg}^Q|qg\rangle + \dots$$
$$|\bar{Q}\rangle = \psi_{\bar{q}}^{\bar{Q}}|\bar{q}\rangle + \psi_{\bar{q}g}^{\bar{Q}}|\bar{q}g\rangle + \dots$$

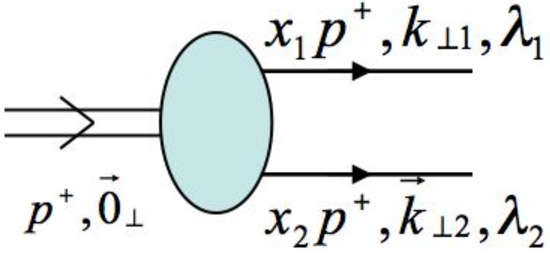

$$\Psi_{Q\bar{Q}}(x_i, \vec{k}_{\perp i}, \lambda_i) = \Phi(x_i, \vec{k}_{\perp i})\chi(x_i, \vec{k}_{\perp i}, \lambda_i)$$

Radial
(Dependent on the model potential)

H = T + V
V includes Coulomb, Confinement, Spin-Spin, Spin-Orbit interactions.

Spin-Orbit
(Interaction independent Melosh transformation)

$$J^{PC} = 0^{++}(f_0, a_0, \dots)$$
$$0^{-+}(\pi, K, \eta, \eta', \dots)$$
$$1^{--}(\rho, K^*, \omega, \phi, \dots)$$
$$\dots$$

PHYSICAL REVIEW C **92**, 055203 (2015)

Variational analysis of mass spectra and decay constants ···

Ho-Meoyng Choi,[1] Chueng-Ryong Ji,[2] Ziyue Li,[2] and Hui-Young Ryu[1]

[1]*Department of Physics, Teachers College, Kyungpook National University, Daegu, Korea 702-701*

[2]*Department of Physics, North Carolina State University, Raleigh, North Carolina 27695-8202, USA*

(Received 15 September 2015; published 13 November 2015)

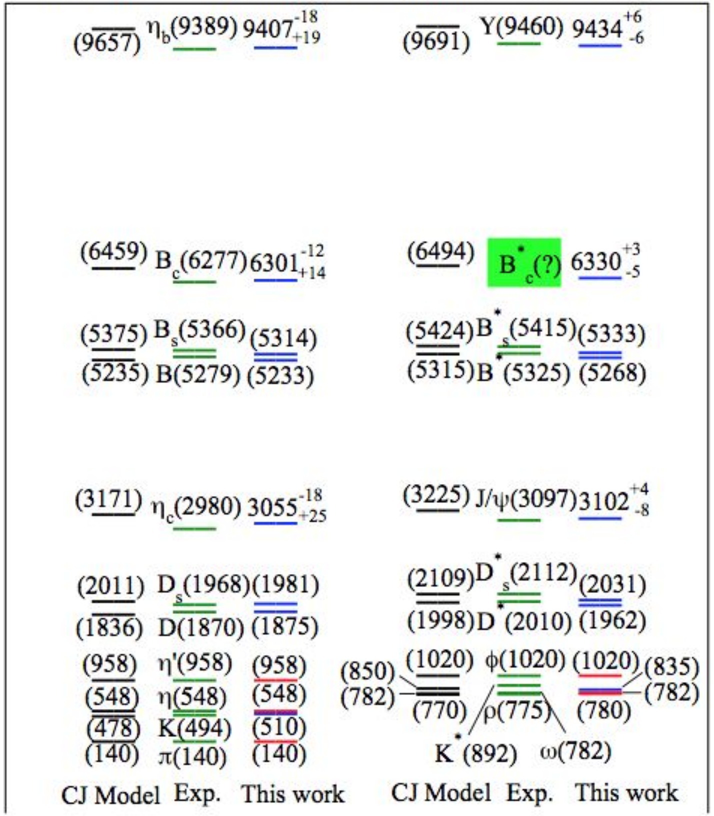

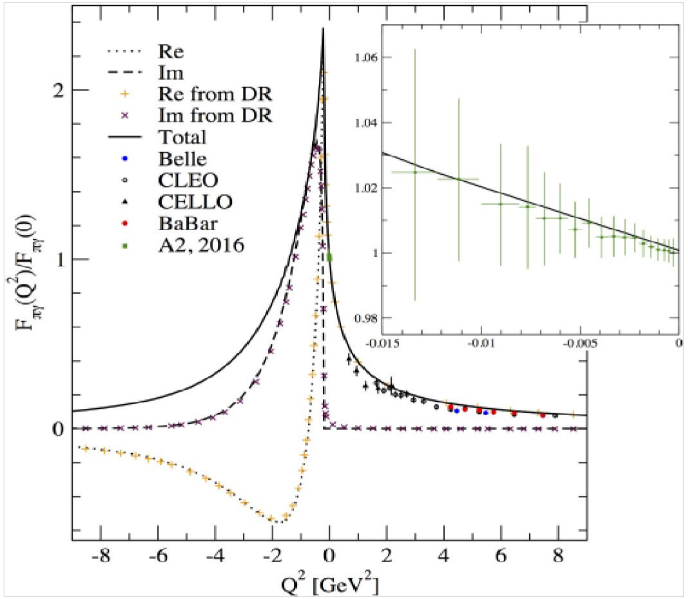

Both spacelike and timelike form factors can be computed in LFQM.

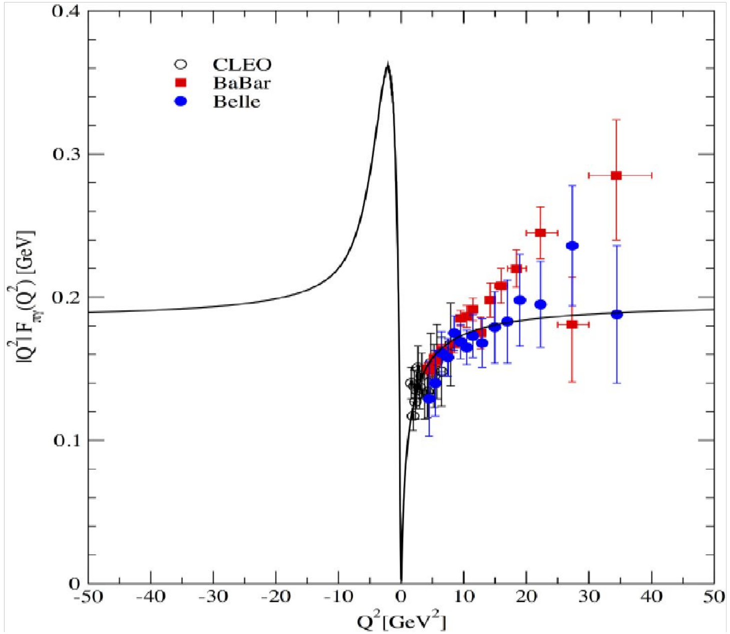

H.-M. Choi, H.-Y. Ryu, C.-R.Ji, PRD96,056008(2017); PRD99,076012(2019)

PHYSICAL REVIEW D **106,** 014009 (2022)

Mixing effects on 1S and 2S state heavy mesons in the light-front quark model

Ahmad Jafar Arifi,[1,*] Ho-Meoyng Choi,[2,†] Chueng-Ryong Ji,[3,‡] and Yongseok Oh[4,1,§]

[1]*Asia Pacific Center for Theoretical Physics, Pohang, Gyeongbuk 37673, Korea*
[2]*Department of Physics Education, Teachers College, Kyungpook National University, Daegu 41566, Korea*
[3]*Department of Physics, North Carolina State University, Raleigh, North Carolina 27695-8202, USA*
[4]*Department of Physics, Kyungpook National University, Daegu 41566, Korea*

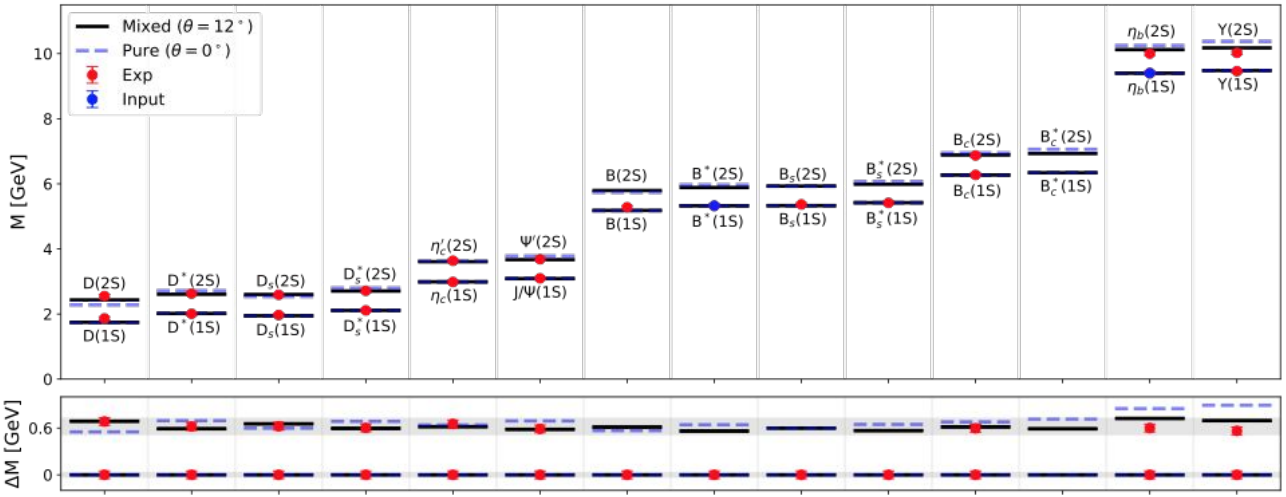

Pseudoscalar meson decay constants and distribution amplitudes up to the twist-4 in the light-front quark model

Ahmad Jafar Arifi,[1,2,3,*] Ho-Meoyng Choi,[4,†] and Chueng-Ryong Ji[5,‡]

[1]*Few-Body Systems in Physics Laboratory, RIKEN Nishina Center, Wako 351-0198, Japan*
[2]*Research Center for Nuclear Physics (RCNP), Osaka University, Ibaraki, Osaka 567-0047, Japan*
[3]*Asia Pacific Center for Theoretical Physics (APCTP), Pohang, Gyeongbuk 37673, South Korea*
[4]*Department of Physics Education, Teachers College, Kyungpook National University, Daegu 41566, South Korea*
[5]*Department of Physics, North Carolina State University, Raleigh, North Carolina 27695-8202, USA*

State	f_{theo}	f_{exp}	State	f_{theo}	f_{exp}
$D(1S)$	208	206.7(8.9)	$D(2S)$	110	⋯
$D_s(1S)$	246	257.5(6.1)	$D_s(2S)$	133	⋯
$\eta_c(1S)$	348	335(75)	$\eta_c(2S)$	214	⋯
$B(1S)$	190	188(25)	$B(2S)$	126	⋯
$B_s(1S)$	228	⋯	$B_s(2S)$	150	⋯
$B_c(1S)$	394	⋯	$B_c(2S)$	268	⋯
$\eta_b(1S)$	628	⋯	$\eta_b(2S)$	443	⋯

Quasi-PDF

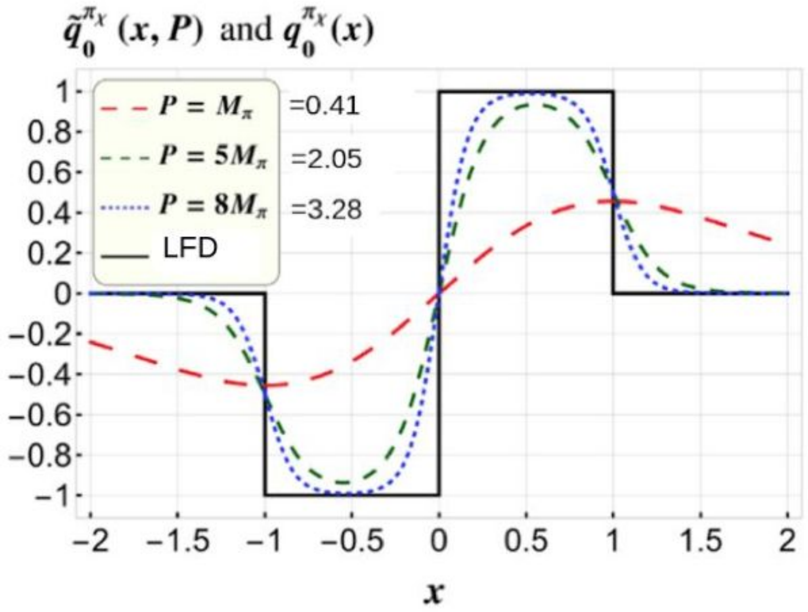

Quark quasi-PDFs and light-front PDF for the chiral pion.

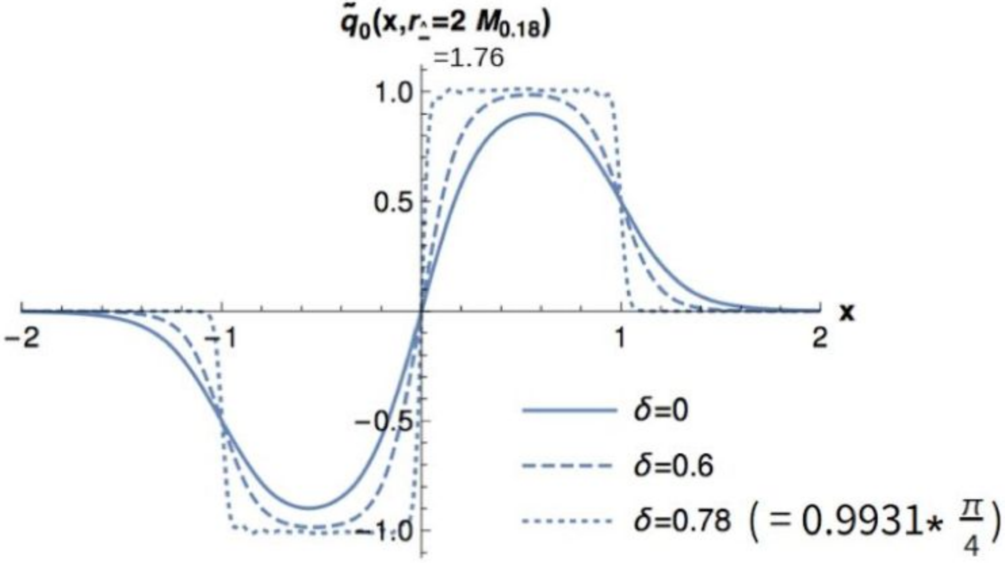

Interpolating "quasi-PDFs" for the chiral pion.

All quantities are in proper units of $\sqrt{2\lambda}$.

Jia, Y., Liang, S., Xiong, X., and Yu, R. (2018). Phys. Rev. D, 98:054011.

Ma, B. and Ji, C.-R. (2021). Phys. Rev. D, 104:036004.

Extended Wick Rotation

$$p^0 \rightarrow \tilde{P}^0 = ip^0 \qquad (\delta = 0)$$

$$For \quad 0 < \delta < \pi / 4 ,$$

$$p^{\hat{+}} / \sqrt{C} \rightarrow \tilde{P}^{\hat{+}} / \sqrt{C} = ip^{\hat{+}} / \sqrt{C} .$$

Correspondence to Euclidean Space

$$p'^2_{\hat{\perp}} = p^2_{\hat{\perp}} / C \leftrightarrow -\tilde{P}^2$$

Conclusion and Outlook

- With the forthcoming EIC and topical collaborations in nuclear theory, the future of hadron physics looks bright.
- Maximal stability group of LFD saves a lot of dynamic efforts.
- Whole landscape between IFD and LFD has been revealed in QED(3+1) and QCD(1+1) with interpolating spinors, gauge bosons and their propagators.
- In particular, QCD(1+1) in large Nc ‘tHooft model provides initial bridge between QCD and LFQM.
- Applying the alternative quasi-PDFs of the interpolating formulation is recommended in the lattice QCD.
- Interpolating QCD(3+1) in Nc=3 between IFD and LFD needs to be explored in particular in the timelike region to study the color confinement.